Sequential coupled numerical simulations of an air/ground-source heat pump: Validation of the model and results of yearly simulations

Sequential coupled numerical simulations of an air/ground-source heat pump: validation of the model and results of yearly simulations

ZANETTI Emanuele[1], BONDUÀ Stefano[2], BORTOLIN Stefano[1], BORTOLOTTI Villiam[2], AZZOLIN[1]* Marco, TINTI Francesco[2]

[1] Department of Industrial Engineering, University of Padova, Via Venezia 1, 35131 - Padova, Italy

[2] Department of Civil, Chemical, Environmental, and Materials Engineering, University of Bologna, Via Terracini 28, 40131 – Bologna Italy

ABSTRACT

Numerical simulations are important tools for the assessment of exploiting geothermal energy in heat pump applications. They can be used to evaluate the performance of the system, the long-term production scenarios and the sustainability of the geothermal reservoir. The present work introduces and describes a numerical model, in which a dedicated Matlab® script has been realized to allow sequentially coupled simulations of a shallow geothermal reservoir and of a heat pump system. A mathematical model of a dual-source heat pump, working alternatively with the ground or the air as heat source/sink, has been developed in Matlab® environment. The heat exchangers of the heat pump have been modelled considering the equations that govern the physical phenomena. The dynamic numerical simulator FEFLOW®, based on the finite element method, has been used to simulate the behaviour of the geothermal reservoir, subjected to heat extraction/reinjection by a closed loop vertical heat exchangers field. This methodological approach is useful to evaluate the performance of the coupled system in the long term, and it is important for understanding the advantages and limits of the dual-source heat pump in assuring sustainability over time avoiding the depletion of geothermal resources. The models and their coupling have been calibrated and validated with experimental data from a shallow geothermal plant located in Tribano (Padova, IT). It consists of eight coaxial borehole heat exchangers 30 m deep, connected to a 16 kW dual-source heat pump prototype. The heat pump system provides heating and cooling to an office area. The coupled model has been used to compare the performance of the heat pump when working in air-mode only or in ground-mode only. This allowed the development of a switching control strategy between the two thermal sources. Yearly simulations with the switching strategy have shown that the seasonal performance factor of the dual-source heat pump during the heating mode can be 13.8% higher compared to the one obtained with a conventional air source heat pump and 3.8% higher with respect to a ground source heat pump.

1. INTRODUCTION

Dual-source heat pumps (DSHPs) can work alternatively with air or ground as heat source/sink and nowadays are seen as an interesting solution because they allow the reduction of the length of the borehole heat exchangers and thus the investment costs. When a DSHP exchanges heat with ambient air, it works as an air-source heat pump (ASHP). On the contrary, when it uses the ground as source/sink it operates as a ground source heat pump (GSHP) following a sequential logic: the heat pump, depending on the building loads, requests an energy amount from the geothermal probes, which exchange heat with the thermal reservoir (Kavanaugh and Rafferty [1]). This process can cause both short and long-term thermal depletion of the reservoir, which must be predicted and managed, to allow the optimal operation of the GSHP system (Focaccia et al. [2]). Numerical simulation is a standard approach in GSHP projects to study the short and long-term thermal depletion of the ground. Indeed, the ultimate purpose is to obtain information to improve and optimize the behaviour over time of the system to increase its efficiency and consequently obtain energy savings (Cui et al. [3]). Many software packages exist to numerically simulate the behaviour of the ground subjected to heat extraction/injection cycles. Some notable case studies of this approach can be found in Al-Khoury et al. [4], Javed and Claesson [5], Pasquier and Marcotte [6], Ruiz-Calvo et al. [7]. The above-mentioned studies focus on the model of the thermal reservoir while they adopt a simplification for the heat pump, which is not modelled and the thermal load exchanged which is defined as a hypothesis. On the other side, there are various models of ground source or dual-source heat pump systems (Li et al. [8], 193, Grossi et al. [9], Lazzarin and Noro [10]) and the TRNSYS simulation tool is widely used [11]. This approach is useful when the main goal is to study the performance of a specific heat pump coupled with a building and its heating distribution system. Often these models rely on the manufacturer's data to determine the behaviour of the heat pump (Hein et al. [12], Li et al. [13]) or on correlations obtained with experimental measurements conducted on the specific heat pump (Corberan et al. [14]). The main drawback of these approaches is that they do not consider the physical phenomena occurring in the heat exchangers and thus they can be applied with difficulty when considering a different refrigerant or different heat exchangers.

It emerges that in the literature there is a lack of works dealing with the modelling of DSHPs that are able to simulate the ground thermal reservoir and the heat pump. The present paper is aimed to cover this gap and presents a new modelling approach that considers the coupling between the numerical model of a shallow geothermal reservoir and the numerical model of a dual-source heat pump. The type of coupling between the two simulators is "sequential", which means that the connection between the two simulators takes place through data files generated by the simulators themselves and managed by a control program. That is, each simulator generates an output data file that is used as

input file for the other simulator in a continuous cycle supervised by an external software layer controlling the correct execution of the coupled simulation and determining its beginning and end. Moreover, the model of the shallow geothermal reservoir is realized with the Finite Element Modeling software package FEFLOW® which is among the most precise and used tools in shallow geothermal design (Diersch [15]) and the model of the heat pump considers the physical equations governing the heat transfer phenomena [16].

The coupled simulator has been calibrated and validated with the experimental data of an existing DSHP with eight geothermal probes installed in Tribano (Padova, Italy) in the framework of the European Project GEOTeCH [17], (see Section 3). Then the coupled simulator has been used to perform yearly simulations of the functioning of the DSHP considering optimum switching strategies between the thermal sources (see Section 4).

2. HEAT PUMP-GEOTHERMAL SHALLOW SEQUENTIALLY COUPLED SIMULATOR

In this Section, the dual source heat pump prototype and the borehole heat exchangers' field are presented. The numerical coupled simulator (DSHP-BHE controller) composed by the combination of the heat pump model and of the shallow reservoir model is described in detail.

2.1 Dual-source heat pump prototype

The prototype heat pump used in this study has been designed for residential applications or small offices: it has a nominal heating capacity equal to 16 kW and it can provide chilled and hot water to satisfy the building's thermal demands. The heat pump is dual source, thus it can work with air or ground as thermal source/sink to absorb or reject heat through a water-to-refrigerant or an air-to-refrigerant heat exchanger. The working refrigerant is R32 (hydro-fluorocarbon refrigerant with $GWP_{100years}$ equal to 677 [18]), which has a global warming potential three times lower than that of R410A commonly used in these applications. The layout of the heat pump is reported in Figure 1. The heat pump is equipped with an inverter-driven scroll compressor that allows to follow the thermal load requested by the user. When the heat pump operates in heating mode (Figure 1a), after the compressor, the refrigerant enters the condenser, which is a brazed plate heat exchanger (BP-HE) and it heats the water of the building distribution system. After the condenser, the refrigerant passes through the electronic expansion valve (EEV) and it evaporates in the finned coil heat exchanger (when using air as thermal source) or in the brazed plate heat exchanger (when using the water from the borehole heat exchanger field as thermal source). When the heat pump operates in cooling mode (Figure 1b),

after the compressor, the refrigerant is condensed in the finned coil heat exchanger (when using air as thermal sink) or in the brazed plate heat exchanger (when using the water from the borehole heat exchanger field as thermal sink). After the condenser, the refrigerant passes through the electronic expansion valve and then produces chilled water in the user brazed plate evaporator. Detailed information regarding the heat pump prototype can be found in [16].

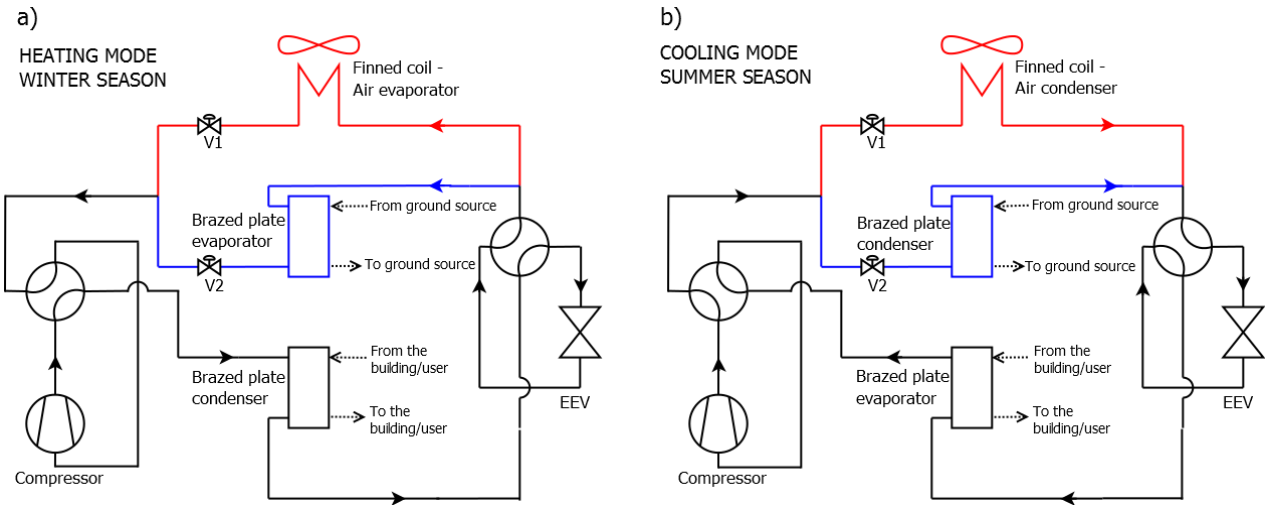

Figure 1 Layout of the dual-source heat pump. a) Refrigerant loop when operating in heating mode (winter season), b) refrigerant loop when operating in cooling mode (summer season). The black solid lines represent the main path of the refrigerant loop, the red solid lines represent the path when using the air source and the blue solid lines represent the path when using the ground source. The solenoid valves V1 and V2 manage to change between the operative modes. EEV is the electronic expansion valve.

2.2 Borehole heat exchangers' field

The borehole heat exchangers' field used for this study includes eight coaxial probes (coaxial borehole heat exchanger - CB-HE), spaced 6 m, down to 30 m deep, without grouting, the latter allowed by local environmental authority of the study area. The shallowest layers are formed by unconsolidated, alluvial soils, with very fine grain size – silt and clay – of low permeability, locally interspersed by sandy layers. The eight CB-HEs are connected in parallel to a central collector and subsequently to the DSHP. The working fluid is pure water. The main parameters of each CB-HE installed are reported in *Table 1*. Besides the eight CB-HEs, three Observation Boreholes (OBs) have been installed to monitor the ground temperature. Further details of the geology and hydrogeology of the area, the monitoring strategy and the system layout can be found in Tinti et al.[19].

Borehole diameter (m)	Inlet Pipe Diameter (m)	Inlet Pipe Wall Thickness (m)	Inlet Pipe Thermal Conductivity (W/(m·K))	Outlet Pipe Diameter (m)	Outlet Pipe Wall Thickness (m)	Outlet Pipe Thermal Conductivity (W/(m·K))
0.15	0.09	0.0029	0.42	0.06	0.0029	0.42

Table 1 Data of each coaxial borehole heat exchanger connected to the DSHP used for the study.

2.3 Heat pump numerical model

The numerical model of the heat pump (named DSHP model) has been developed in Matlab® environment and it considers all the components of the heat pump to simulate its operation during steady-state conditions. In particular, the models of the heat exchangers have been developed considering a finite discretization over their volume and each discretized element as an independent heat exchanger where continuity, momentum and energy equations are solved. This approach allows the model to be flexible and to estimate the performance of heat pumps operating also with various heat exchanger geometries and refrigerants.

When considering the model of the finned coil heat exchanger (FC-HE), its volume is subdivided into identical elements which are sequentially treated following the refrigerant path. For each $i-th$ element, the refrigerant outlet condition is calculated based on the ε-NTU method. The effectiveness of the heat exchanger is defined as:

$$\varepsilon_i = Q_i / Q_{max,i} \qquad \text{Eq. (1)}$$

where Q_i is the heat flow rate exchanged in the tube element and $Q_{max,i}$ is the maximum heat flow rate that can be exchanged in a perfect counter-current configuration with an infinite heat transfer area. The Number of Transfer Units (NTU_i) of the tube element depends on the $(U_i A_i)$ product, where A_i is the heat transfer area and U_i is the global heat transfer coefficient:

$$U_i = \frac{1}{1/HTC_r + R_{cd} + 1/HTC_{air}} \qquad \text{Eq. (2)}$$

where HTC_r and HTC_{air} are the local heat transfer coefficients of the refrigerant and of the air and R_{cd} is the thermal conduction resistance of piping and fins.

The air-side heat transfer coefficient is calculated through the equations of Rich [20] and a modeling of the air dehumidification has also been implemented following the procedure proposed by Threlkeld [21]. On the refrigerant side, when the finned coil works as the condenser, the heat transfer coefficient has been evaluated with the Cavallini et al. [22] correlation which has been proved in various works to give good predictions even with small diameter channels and when using R32 (Azzolin et al.[23], Azzolin and Bortolin [24], Matkovic et al. [25]). When working as the evaporator, the refrigerant heat transfer coefficient is calculated with the Liu and Winterton [26] equation. The Dittus-Boelter equation for the heat transfer coefficient has been used in the zones of the heat exchanger where the refrigerant is single phase (desuperheating and subcooling regions in the condenser and superheating region in the evaporator). Finally, the approach of Webb [27] has been adopted for the condensation in superheated vapor. Once the equations for all the discretized elements have been solved using a guessed value of the evaporation/condensation temperature,

the refrigerant outlet conditions obtained by the sequential calculations are compared to the desired values of the outlet superheating/subcooling. Based on this comparison, the condensation/evaporation pressure is updated, and the process repeats until convergence.

In the model of the BP-HEs, the total volume of a representative plate of the heat exchanger is subdivided into various elements of different sizes. First, some macro-regions ($re-th$) are identified based on the refrigerant heat transfer process (desuperheating, condensation and subcooling for the BP-HE condenser; evaporation and superheating for the BP-HE evaporator). Each $re-th$ region is subdivided into discrete elements where the same amount of heat Q_{re} is transferred. Indeed, with this approach, the heat to be transferred in each element is known and this allows to calculate the $j-th$ heat transfer area (for a $j-th$ discretized element pertaining to the $re-th$ region) with the following relationship:

$$A_j = \frac{Q_{re}}{U_j \cdot \Delta T_{ml,j}} \qquad \text{Eq. (3)}$$

where A_j and U_j are the heat transfer area and the global heat transfer coefficient, respectively; $\Delta T_{ml,j}$ is the logarithmic mean temperature difference.

Regarding the BP-HE condenser, the heat transfer coefficient for the single-phase regions (refrigerant in the desuperheating and subcooling zone and also water) has been calculated with the Martin [28] correlation for single-phase, while in the condensation of saturated vapour region, the refrigerant heat transfer coefficient has been evaluated with the equation proposed by Longo et al. [29] (the Webb approach [27] is used for the condensation in the superheated region). When the BP-HE works as evaporator, the heat transfer coefficient for the single-phase regions is calculated with the Martin [28] correlation and the refrigerant heat transfer coefficient in the two-phase zone is calculated with the Amalfi et al. correlation [30].

Once the area of each element is determined, the overall heat exchanger surface is computed as a summation over all the elements and it is compared with the real BP-HE surface considering the following ratio:

$$r = \frac{\sum A_j}{A_{BP}} \qquad \text{Eq. (4)}$$

where A_{BP} is the effective BP-HE heat transfer area. The condensation/evaporation pressure is thus updated until r reaches a value close to unity.

Regarding the compressor, a specific subroutine has been developed: it includes the polynomial maps of the compressor according to the reference standard [31]. These polynomials manage to calculate the corresponding power

consumption and mass flow rate, which is an input for the heat exchangers subroutines. More information about the compressor model can be found in [16].

The schematic flow chart of the iterative algorithm of the model is displayed in Figure 2.

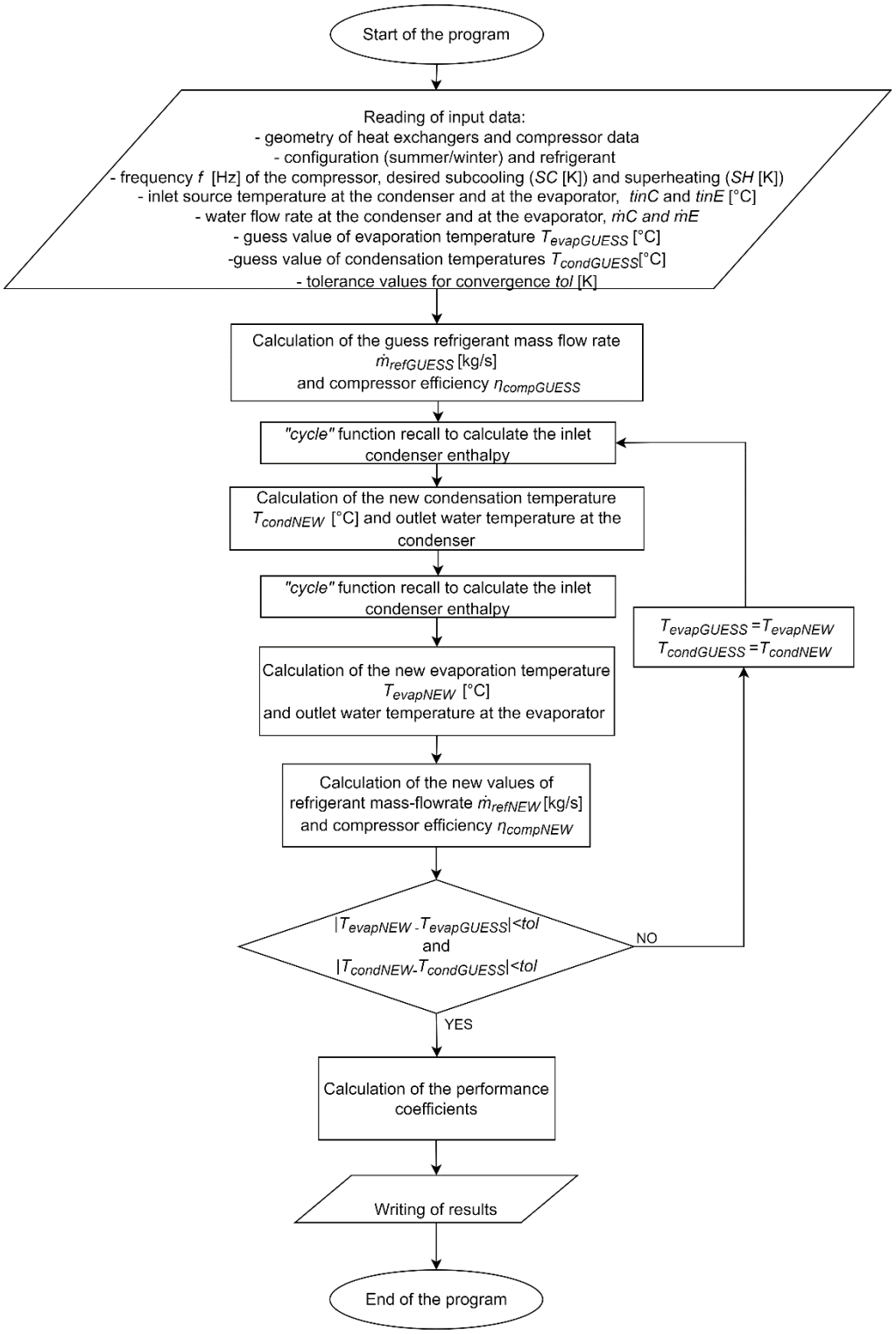

Figure 2 Flow chart of the algorithm of the DSHP model.

The required inputs of the DSHP model are: the compressor frequency (f); mass flow rate and the water temperature ($T_{USERout}$) on the user side; mass flow rate and temperatures (T_{BHEout} or T_{AIRout}) of the external source/sink (no temperature differences are assumed between T_{BHEout} and the inlet temperature at the ground brazed plate heat exchanger); the refrigerant subcooling temperature at the condenser outlet (SC); the refrigerant superheating temperature at the evaporator outlet (SH); first attempt values for the condensation and evaporation temperatures ($T_{evapGUESS}$, $T_{condGUESS}$). The algorithm starts with the calculation of first attempt values of the compressor efficiency ($\eta_{compGUESS}$) and refrigerant mass flow rate ($\dot{m}_{rGUESS}$) by means of the compressor subroutine. After determining all the initial values, an iteration cycle begins and at each iteration, new values for condensation/evaporation pressure, compressor efficiency and refrigerant mass flow rate are provided by the models described above. During the runtime, a particular subroutine called "cycle" is recalled and it is used to solve the refrigerant thermodynamic cycle, i.e. calculate the refrigerant conditions (enthalpy at the inlet-outlet of each component) based on the partial results. The entire procedure stops when the condensation/evaporation temperatures reach convergence values.

2.4 Geothermal shallow reservoir numerical model

In order to evaluate the behaviour of geothermal probes exchanging heat with the ground, a dynamic simulator is necessary. In this specific application, the software FEFLOW® (Finite Element Flow simulator) has been chosen, which has a dedicated section for modelling and simulating Borehole Heat Exchangers (BHEs) and allows the definition of the hydrogeological modelling of the studied area. The numerical model implemented is based on Al-Khoury ([32,33]) and includes specific equations for various types of BHE. A finite element formulation is derived for describing both steady and transient states of heat transfer between the BHE and the ground. The conservation of mass in groundwater flow and the continuity of energy for heat flow are included as governing differential equations for 3D systems. FEFLOW® can operate fully transient simulations and allows the realization of as many layers as needed and upload from a database of thermophysical, petrophysical and physical information for each layer (thermal conductivity, thermal capacity, hydraulic conductivity, temperature). This is important because in this application the vertical temperature gradient around the BHEs varies in time, subjected to both weather conditions and heat exchanged with the heat pump. In the specific case, the model domain implemented extends around the CB-HEs field, for a total surface area of 50 x 78 m^2 and a depth of 44 m [34]. A tetrahedral mesh was used with refinement regions around the eight CB-HEs. A set of observation points have been inserted in correspondence of the three OBs installed to monitor the undisturbed and disturbed ground temperature. A series of nine layers was used to detail the geology of the area. Layer 1 is a buffer

layer on the top, introducing the weather impact boundary condition, while Layers 2-8 cover the length of the CB-HE, 30 m, and finally Layer 9 guarantees the existence of a geothermal heat flow from the bottom. The impact of ambient weather down with depth, and its variation across seasons, was added at the borders of the model, as temperature boundary conditions, varying with depth and time. A difference in the hydraulic head from 1.5 m (top right corner) to 1.6 m (bottom left corner) takes into account the groundwater flow movement, according to the available hydrogeological information. Estimated values of ground properties, such as the hydraulic conductivity (1 m/d), the effective porosity (30%), the thermal conductivity (3 W/(m K)) and the heat capacity (2.5 MJ/(m^3·K)) have been used in the model according to the information acquired from hydrogeological studies (Tinti et al., 2018 [19]). The ground natural state is provided by simulating the thermal state of the model, without activation of the CB-HE for several years, and then validating the temperature results in the nodes corresponding to the measurement points of the three OBs. Temperature values at the nodes among the measured values and the CB-HEs are calculated by linear interpolation for each depth.

2.5 Coupled simulator: Matlab script allowing sequential coupled simulation

To simulate all the possible operative modes of the heat pump, a DSHP-BHE controller has been developed in MATLAB® to link the DSHP model and the model of the BHEs. The schematic of the system, including the common variables between the two models, is displayed in Figure 3a. The controller is able to run transient simulations of the system and its inputs are the external air temperature, the initial ground temperature distribution (which can be either natural state, or already thermally disturbed condition including the BHE field), the speed of the compressor and the operative mode. The controller can manage three possible operative modes:

- System operating as a Ground source heat pump (GSHP). In this case, the ground is the only thermal source/sink and the refrigerant flows through valve V2 to the ground plate heat exchanger that can work as condenser or as evaporator. The conceptual model of the coupled simulation in GSHP mode is presented in Figure 3b. As the first step, the temperature of the water returning from the ground T_{BHEout} is initialized. Then, the DSHP model runs, and the heat flow rate exchanged at the ground BP-HE is calculated. The water temperature at the outlet of the ground BP-HE, $T_{DSHPout}$, is calculated with the DSHP model and used as input for the BHE model (FEFLOW® simulator). The FEFLOW® simulation runs and its output (heat flow rate exchanged with the ground and T_{BHEout}) is then used as new input data for the DSHP numerical simulation in the subsequent time step together with the updated values of the compressor speed. Since each FEFLOW® run provides many

temperature results at smaller steps, the average value in the period is taken as output for the required time. This procedure repeats for all the defined time steps and, at the end of the simulation period, the coupled simulator reports the final results in .csv format. It is worth mentioning that when the thermal load is null (compressor frequency equal to zero), the governing differential equations related to the ground and to the BHE are still solved. In this case, the boundary conditions are represented by the varying air temperature and undisturbed ground temperature.

- System operating as an Air source heat pump (ASHP). In this case, the air is the only thermal source/sink and the refrigerant absorbs/releases heat to the ambient through the finned coil heat exchanger. When operating in ASHP mode, the controller runs the DSHP model in every time step, providing as input the air temperature and compressor speed until the end of the simulation period.

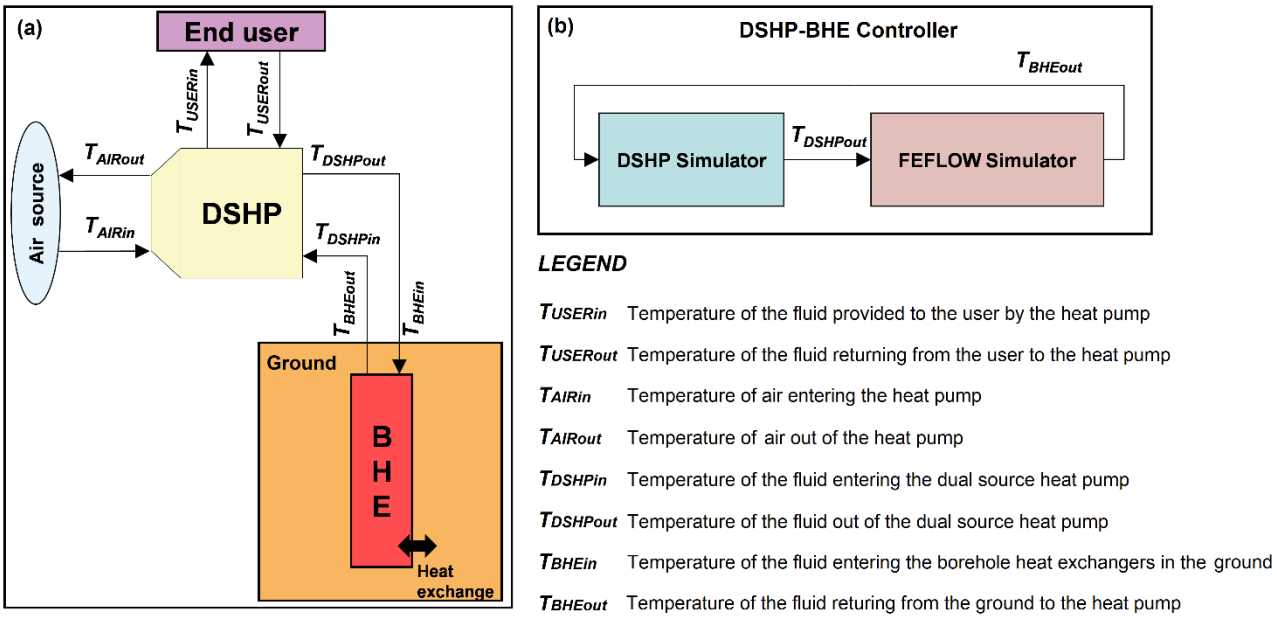

Figure 3 Conceptual model of the coupled simulation: (a) general model of the inputs and outputs of the system; (b) detail of the DSHP-BHE controller operating in GSHP mode.

- System operating as a dual source heat pump (DSHP). In this case, the workflow of the DSHP-BHE controller is presented in detail in Figure 4. The controller has to manage the switch between the ground mode and the air mode. In ground mode, the DSHP model and FEFLOW® run sequentially according to the schematic of Figure 3b. When operating in air mode, both models are run by the controller, too. The governing equations of the ground and BHE field are always solved to update the state of the ground even without working fluid circulation and if the system is operating as an ASHP. All the transient phenomena occurring in the heat pump (e.g., when the compressor is powered on or switched off) are not considered because the thermal inertia of the heat pump is negligible compared to that of the building and of the ground.

When the system operates as a DSHP, the following additional controls are also applied: the difference between the air and temperature of the fluid at the BHE outlet $T_{air} - T_{BHEout}$ is used as control parameter to decide which is the thermal source that allows to reach higher performance (more details on this are given in the Section 4.3 with a dedicated analysis); the water temperature from the BHE field (T_{BHEout}) should be higher than 4 °C otherwise the DSHP switches to air mode to avoid freezing problems (since this system should operate without glycol).

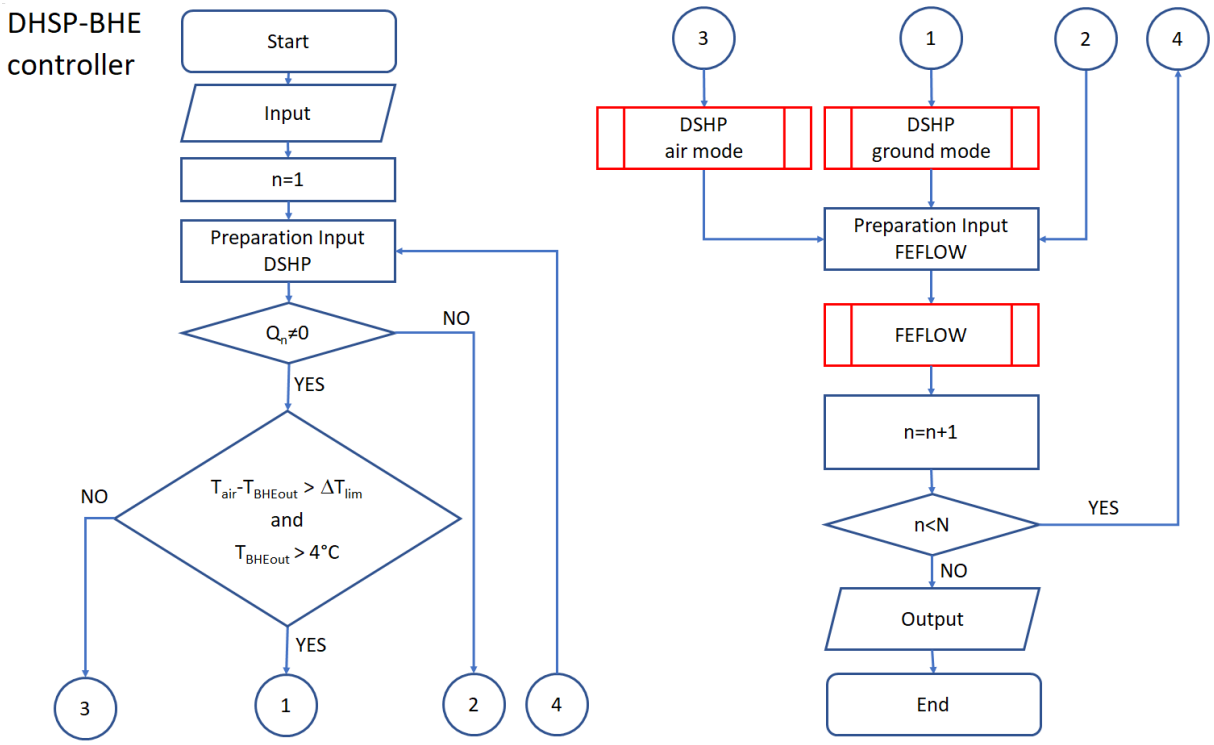

Figure 4 Workflow of the DSHP-BHE controller allowing the coupled simulation when operating in DSHP mode.

3. VALIDATION OF THE SEQUENTIAL COUPLED SIMULATOR

The model of the heat pump considering the physical equations governing the heat transfer phenomena (hereinafter "thermodynamic DSHP model") and the finite element model of the ground have been validated separately in previous works and proved to be accurate to predict the performance of the heat pump and the behaviour of the borehole heat exchanger field. The validation of the DSHP model with experimental data in several operative conditions can be found in [16]. The DSHP model was able to predict the coefficient of performance of the heat pump within ±10% both when considering heating and cooling modes. Regarding the model of the BHE implemented in FEFLOW®, multiple tests and comparisons with experimental results by many authors have shown the model to be quite robust in predicting the heat exchanged in a GSHP system (Nam et al. [35]), simulating the aquifer thermal plumes and their effect on the BHE closed-

loop applications (Rivera et al. [36]). Finally, it has been used as a benchmark for evaluating the performance of other modelling tools (Nam and Ooka [37]). Specifically to the FEFLOW® model of the CB-HE field installed in the Tribano area, the validation was performed comparing the simulated temperature changes in the ground nodes with the measured values from the monitoring points in the three observation boreholes, which can be found in [19]. The details of the model realized in FEFLOW® can be found in [34].

However, a validation of the sequential coupled model against experimental data is needed in order to calibrate the coupled model, and it is presented in this Section.

3.1 Demo site characteristics and BHE model implementation

The end-user of the dual-source heat pump system described in Section 2.1 is an office building in Tribano, located in the alluvial Po Plain (45°12′ 32′′ N 11°50′ 44′′ E). The DSHP started working in November 2017 and, after a testing period, it became fully operational in summer 2018 providing heating and cooling to the building.

The map of the system including the building, the heat pump and the CB-HE configuration is reported in Figure 5. During a preliminary monitoring activity, it has been seen that the hydraulic distribution system of the CB-HE field was not balanced since the length of the pipes between the collector and each BHE was different. Therefore, it is not possible to operate with the hypothesis of perfect distribution of the total water mass flow rate among the different probes. This specific problem has been addressed in [38] and to account for the different distributed and concentrated pressure losses, different multiplication factors are used to calculate the fraction of water mass flow rate that flows in a specific probe. The fractions of each probe are reported in Table 2.

The DSHP is instrumented and equipped with a remote controller thus all main parameters and variables of DSHP are monitored. In particular, all the temperatures and pressures at the inlet/outlet of the various components, water mass flow rates in the heat exchangers and power consumptions are acquired every 2 minutes.

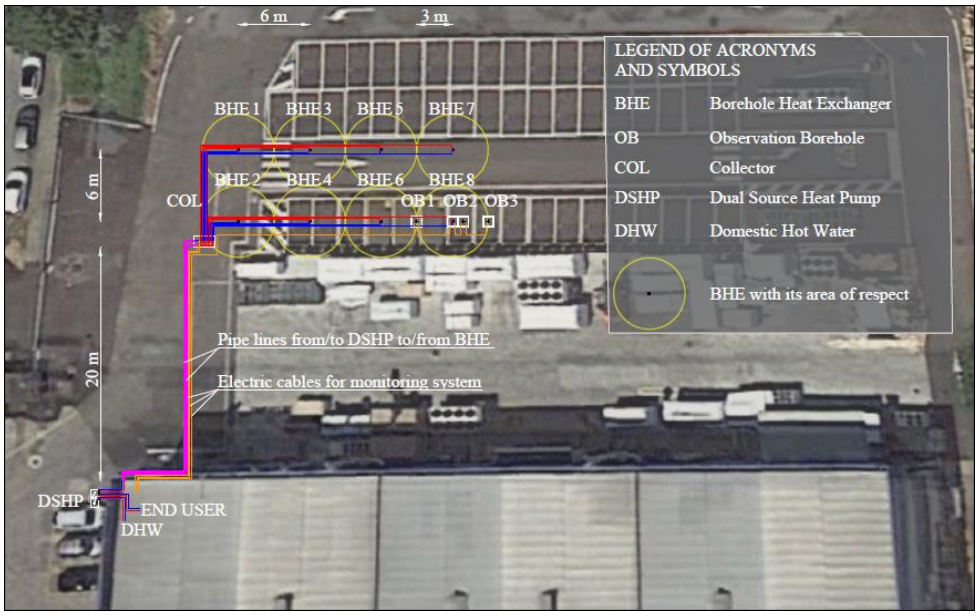

Figure 5 Map and scheme of the case study. Superimposition with Google Earth® satellite image

Borehole	CB-HE1	CB-HE2	CB-HE3	CB-HE4	CB-HE5	CB-HE6	CB-HE7	CB-HE8	TOTAL
Fraction [-]	0.142	0.193	0.116	0.142	0.101	0.116	0.09	0.101	1

Table 2 Fraction of Mass Flow Rates in the eight CB-HEs

3.2 Coupled model validation against experimental data

The validation of the coupled model has been realized considering the experimental data taken during the winter and the summer season.

As regards the winter data, five days of real system operation have been considered starting from 28th January 2019. Figure 6 reports, for the five days, the experimental heating capacity measured at the condenser (which is the thermal load required by the building) and the experimental frequency of the compressor, which is the input to the DSHP model. It can be noticed that the compressor operates mainly during the daytime, when the employees are in the office, while during the night, the compressor works mainly at the minimum frequency, equal to 30 Hz, and it turns on and off to satisfy the lower thermal demand.

The compressor frequency has been used as input to the coupled model to simulate the performance of the system during the five days with a time step equal to 30 minutes. The monitored ground temperature in the three OBs for the 28th of January has been used to reconstruct the initial state of the ground and to assign the input values to the corresponding nodes of the mesh. The temperatures in the remnant nodes have been calculated by linear interpolation. Figure 7 reports the comparison between the measured and the calculated inlet/outlet water temperature circulating

in the BP-HE condenser. The model provides accurate results and the average absolute temperature difference between the measured and simulated values is equal to 0.52 °C for the T_{BHEin} and 0.46 °C for the T_{BHEout} considering all the N time steps. The averaged absolute temperature difference has been calculated with the following equation:

$$T_d = \frac{\sum|T_{BHE-sim} - T_{BHE-meas}|}{N} \quad \text{Eq. (5)}$$

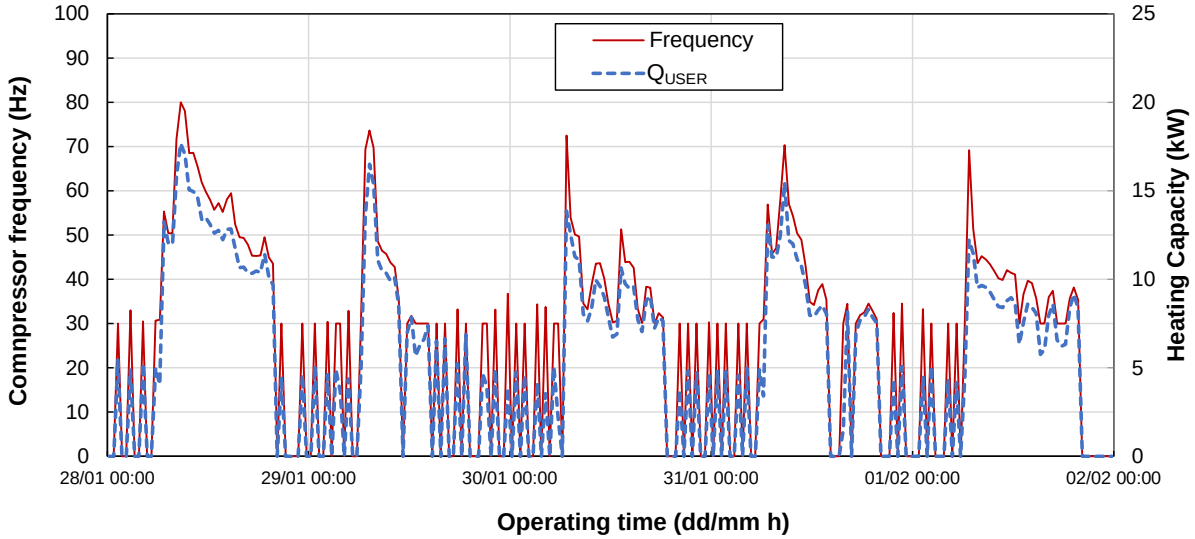

Figure 6 Frequency of the compressor and heating capacity (Q_{USER}) during the five winter days considered for the coupled simulator validation.

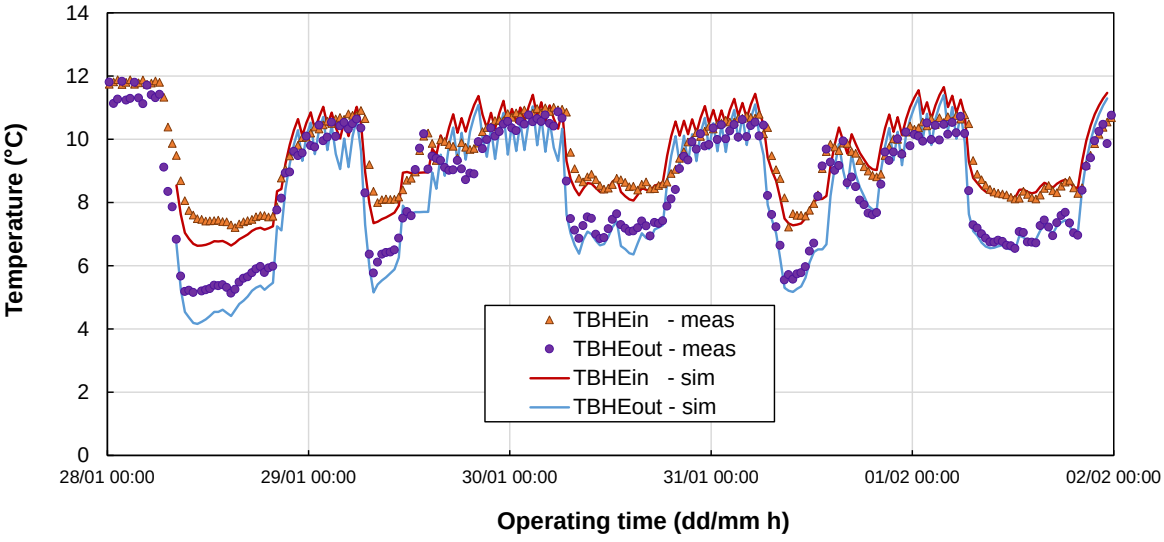

Figure 7 Comparison between experimental and numerical data of water temperature circulating in the BHE during the five winter days considered for the coupled simulator validation. Points: measured data, lines: calculated data.

The validation of the coupled DSHP-BHE model has been realized also considering the summer period (when the building requires cooling capacity for the air-conditioning system) by simulating five days of real system operation starting from the 30th of July 2019. As for the simulations in the heating period, the time step was fixed to 30 minutes and the inputs

were: the compressor frequency, the mass flow rate of water in the secondary loops, the air temperature and the temperature of the water coming from the building (considered equal to that entering the evaporator). Figure 8 displays the experimental compressor frequency and the cooling capacity at the evaporator). Similarly to the winter data, the cooling demand is higher during the daytime due to the presence of people in the office while during the night the compressor is turned off most of the time.

Figure 9 reports the comparison between the calculated and measured values of the inlet/outlet temperature of the water circulating in the BP-HE evaporator. The results were found to be in good agreement with the experimental data. In particular, the average absolute temperature difference between the measured and simulated values is equal to 0.48 °C for the T_{BHEin} and 0.99 °C for the T_{BHEout}.

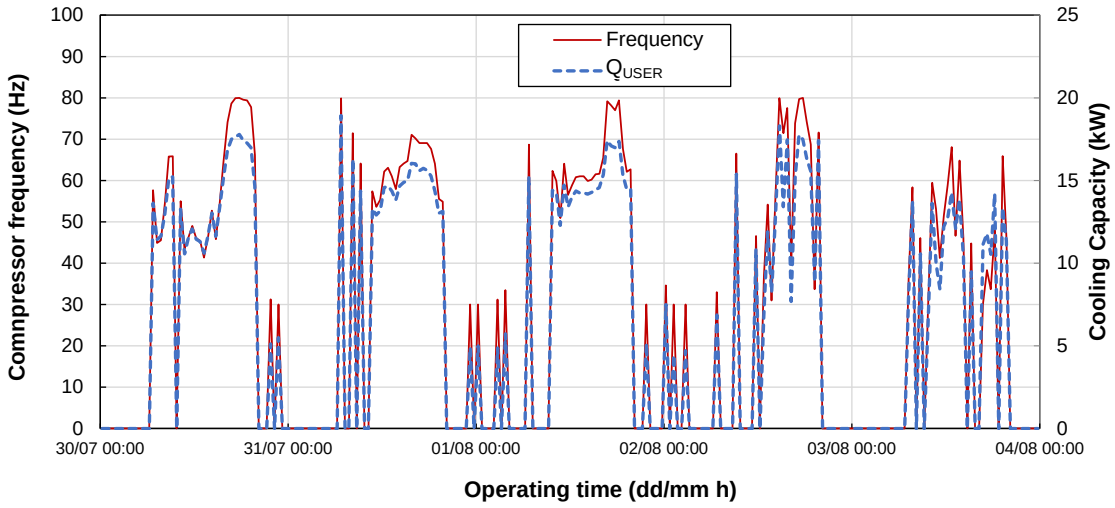

Figure 8 Frequency of the compressor and cooling capacity (Q_{USER}) during the five summer days considered for the coupled simulator validation.

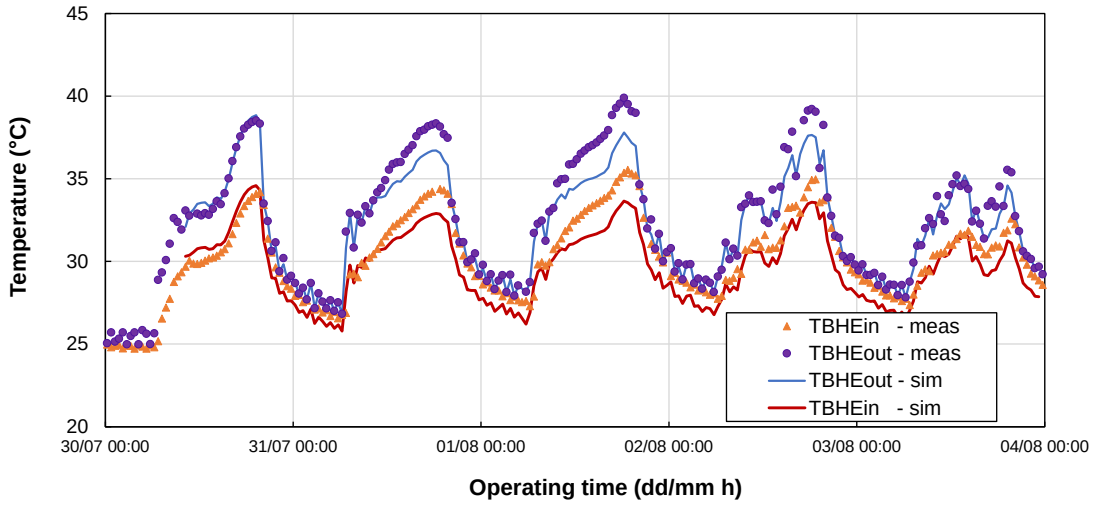

Figure 9 Comparison between experimental and numerical data of water temperature circulating in the BHE during the five summer days considered for the coupled simulator validation. Points: measured data, lines: calculated data.

3.3 Use of LUTs to reduce the simulation time

When performing yearly simulations, the coupled model is time-consuming because the DSHP model and the BHE model have to perform several iterations for each time step. In order to reduce the simulation time for the yearly calculations, the DSHP model has been used to create look-up tables (LUTs) containing the main performance indicators (i.e. heating/cooling capacity, condensation/evaporation temperatures, coefficient of performance). The LUTs have been obtained by cubic interpolation of data simulated with the DSHP model running alone. The simulations with the DSHP model have been done by varying the compressor frequency and the water temperature from the BHE. Lookup tables have been created also when the heat pump operates with the air as thermal source/sink varying the compressor frequency, the fan velocity, the air temperature and humidity. The parameters and the operational range used for the construction of the LUTs are reported in Table 3. To verify the accuracy of the LUTs, the results obtained with the DSHP model using the look-up tables have been compared with the results obtained with the DSHP model at some conditions that have not been used for LUT construction (and reported in Table 3). The results of this comparison are reported in Figure 10 in terms of cooling/heating capacity and performance coefficients (EER, COP) which are calculated as the ratio between the cooling/heating capacity Q and the heat pump power consumption P:

$$\mathrm{EER}\,,\mathrm{COP} = \frac{Q}{P} \qquad \text{Eq. (6)}$$

The data in Figure 10 refer to simulations realized at compressor speed equal to 40, 60 and 80 Hz, fan velocity equal to 60% of the maximum rate, T_{air} and $T_{DSHPout}$ equal to 30.5 °C (summer simulations) and 10.5 °C (winter simulations) respectively. It can be observed that the deviations between the results obtained with the thermodynamic DSHP model and those obtained with the LUTs are always below 1%. It can be concluded that the LUTs derived by the thermodynamic DSHP model are useful to reduce the simulation time when performing yearly simulations without sacrificing the accuracy. Thus, the results of the yearly simulations reported in Section 4 have been obtained with the LUTs.

It is important to stress that differently from the DSHP model presented in Section 2.1, the LUTs used for the yearly simulation do not take the compressor frequency as an input, but the heating or cooling power requested by the user and that has to be provided by the DSHP. All the other outputs are the same of the DSHP model, i.e. the evaporation/condensation temperature, refrigerant mass flow rate, conditions of the source fluid entering the DSHP (air or ground water), power consumptions and performance coefficients.

	Compressor frequency (Hz)	Fan velocity (%)	T_{air} Cooling (°C)	T_{air} Heating (°C)	RH_{air} (%)	$T_{BHE,out}$ Cooling (°C)	$T_{BHE,out}$ Heating (°C)
Min	30	30	25	-5	0	4	12
Max	90	90	40	25	100	20	40
Step	20	20	1	1	20	1	1

Table 3 Input range selected for the creation of the look-up tables based model of the DSHP. The table reports both the environmental conditions (air and ground water conditions) and the operative conditions of the heat pump (compressor frequency and fan speed) for the various modes (heating or cooling).

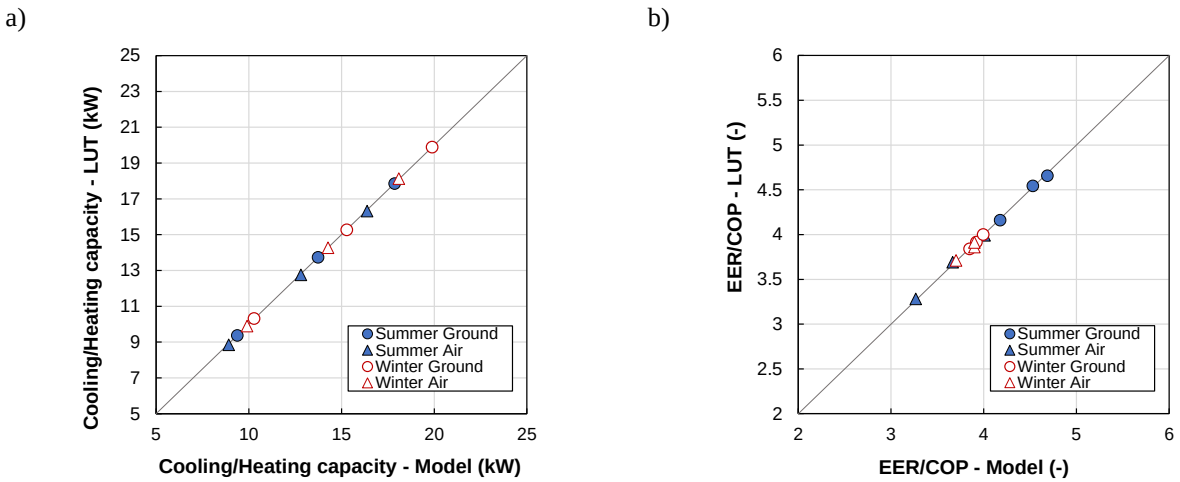

Figure 10 Comparison between the results obtained by the DSHP model and the values provided by the LUTs. Cooling/Heating capacity a) EER/COP b).

4. YEARLY SIMULATIONS

The coupled model has been used to perform yearly simulations of the functioning of the DSHP-BHE system. Since the DSHP can work both with the air or the ground as the thermal source/sink, this raises the problem of how to manage the two thermal sources to maximize the performance of the system.

4.1 Yearly simulation results: performance of the DSHP when working as an ASHP or as a GSHP

In this Section, the results of the first set of simulations are presented: these simulations have been done considering the dual-source heat pump working as an ASHP (air as the only source/sink) or as a GSHP (ground as the only source/sink) for the whole year. The simulations of the heat pump working in air mode consider the fan velocity that guarantees the maximum hourly COP of the system.

To perform the yearly simulations, the hourly weather data for the city of Tribano have been provided by the Regional Environmental Authority ARPAV [39]: the average air temperature was equal to 13.9 °C, minimum temperature equal

to -8 °C and a maximum temperature equal to 37.9 °C. The space heating of the building is supposed to work only when the external temperature is below 18 °C in the period from the beginning of November to the end of March and it is active during the daytime from 7 AM to 7 PM (12 h operation). The nominal space heating load is equal to 15 kW at the design point which is defined considering an external temperature equal to -5 °C; the thermal load decreases linearly for higher external air temperatures [40]. It is assumed that during the heating season the water enters the user heat exchanger of the heat pump at 40 °C and exits at 45 °C. The air-conditioning system of the building is supposed to work only when the external temperature is above 25 °C in the period from the beginning of May to the 15th of September during the daytime from 7 AM to 7 PM (12 h operation). The cooling load increases linearly with the external temperature from 25 °C to 38 °C, the maximum cooling load is equal to 15 kW. It is assumed that during the cooling season the water enters the user heat exchanger at 12 °C and exits at 7 °C. The minimum heating/cooling thermal load required by the building was set equal to 10 kW. The yearly simulations start from the 28th of January, when the reconstructed natural state of the ground was available and used for the model validation (see Section 3.2). When performing the ground mode simulation, the water mass flow rate on the ground loop was considered to be constant and equal to 3900 kg/h.

Figure 11 reports the air temperature T_{air} during the year and the temperature difference between the external air and the water coming from the BHE field ($T_{BHEout} - T_{air}$) calculated from the simulation with the heat pump working as GSHP. The temperature values are reported as simple moving average within 24 hours. It can be observed that during the cooling season T_{BHEout} is always lower than T_{air}, being on average 3.2 K lower. The result of this is that in the summer period the heat pump working as ASHP will be less efficient compared to the GSHP. Indeed, during the cooling season, the mean coefficient of performance obtained with the GSHP is almost twice the one obtained with the ASHP. Considering the seasonal performance factor (SPF) is defined as:

$$SPF = \frac{\sum Q_n \cdot \Delta t_n}{\sum P_n \cdot \Delta t_n} \qquad \text{Eq. (7)}$$

where $Q \cdot \Delta t$ represents the hourly cooling/heating provided by the DSHP (i.e. the thermal load Q_{USER}) and $P \cdot \Delta t$ is the corresponding energy consumption. During the cooling season, the SPF in ground mode is equal to 7.75, while in air mode is equal to 4.26.

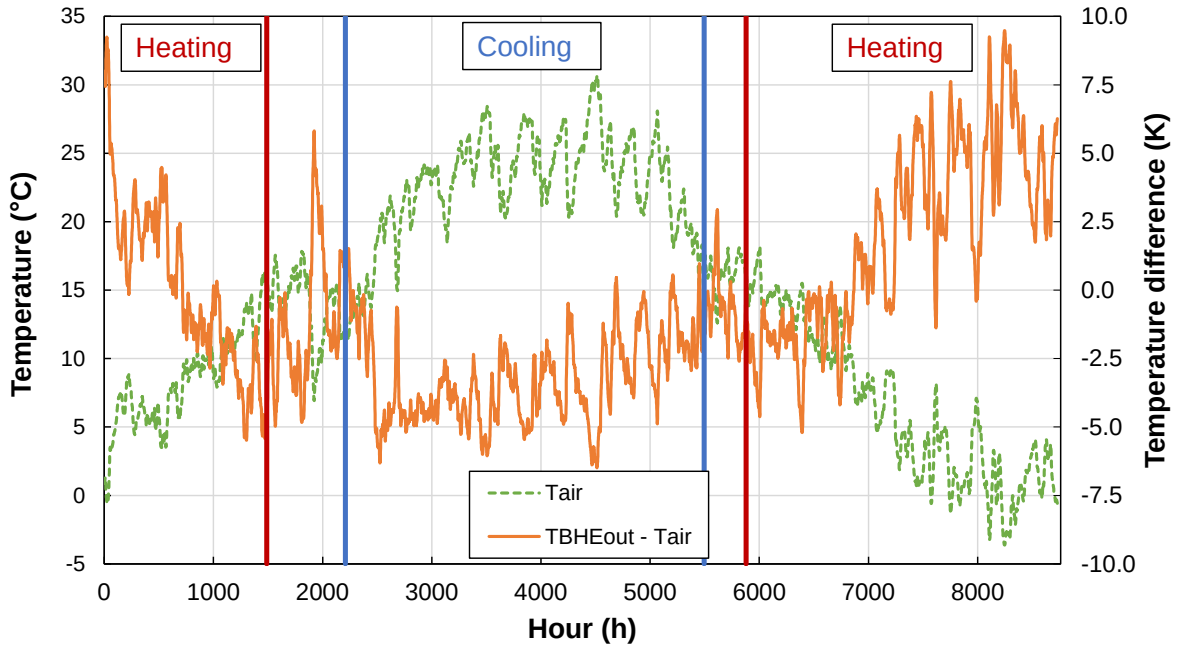

Figure 11 Air temperature during the yearly simulation (orange straight line). Difference between ground temperature (water entering the heat pump from the ground loop) and air temperature in the case of the heat pump working in GSHP mode (blue dotted line). The data reported are the simple moving average within 24 hours.

In heating mode, the mean hourly performance coefficient when the heat pump operates with the ground source is equal to 3.70 and when the air source is used, it is equal to 3.62. The seasonal performance coefficient is 9.8% higher for the GSHP compared to the ASHP (SPF=4.26 in ground mode, SPF=3.88 in air mode). However, when this system operates for the whole winter season in ground mode, T_{BHEout} tends to progressively decrease during the year reaching temperatures below the antifreeze temperature limit (less than 4 °C). This means that for the present case study of shallow borehole heat exchangers it would not be possible to work only in ground mode without using the antifreeze addition (to secure the correct and safe work of the system).

4.2 Control strategy and results of coupled simulations

As reported in the previous Section, the performance of the present heat pump prototype working in ground mode-only is higher compared to the air mode-only operation when considering the summer season (cooling period). During the winter season (heating period), the use of this undersized CB-HE field is not always convenient, leading to low water temperatures inside the BHEs. Furthermore, from Figure 11 it can be observed that in mid-season periods when heating is required, the air temperature (moving average) is higher than ground temperature by more than 2 K, meaning that the functioning in air mode can still be a valid alternative. In order to exploit both the air and the ground source, it is possible to operate in dual source mode and this will allow to achieve a double benefit:

- increase the performance of the heat pump compared to the case of working in air-only or ground-only mode.
- reduce the temperature drift of the ground and avoid low temperature of the water returning from the ground with the risk of freezing.

However, this poses the problem of how to manage the two thermal sources and to decide a control strategy to switch between them to maintain high efficiencies. The results of the simulations in air-only mode and ground-only mode have been used to develop a switching strategy for the heating season. Figure 12 reports the hourly COP difference ($COP_{air} - COP_{ground}$) as a function of the temperature difference between the two sources ($T_{air} - T_{BHEout}$) obtained from the simulations in air-only mode and ground-only mode. It can be observed that the COP difference is well correlated with the temperature difference as a linear function; on average, COP_{air} is higher than COP_{ground} when the air temperature is higher by 1.6 K than the temperature of the water returning from the BHE field. This temperature difference is an effective parameter that can be also easily implemented in the real controller of the heat pump system. Regarding the control strategy in the model, when the temperature difference reported in Eq. (8) is higher than $\Delta T_{lim} =$ 1.6 K, the heat pump operates in air mode otherwise it operates in ground mode.

$$(T_{air} - T_{BHEout}) > \Delta T_{\mathrm{lim}} \qquad \text{Eq. (8)}$$

It must be mentioned that the controller manages to switch to air mode also during the periods when the water returning from the ground reaches values less than 4 °C (T_{BHEout} < 4 °C): in this case, the objective is to avoid excessive degradation of the heat pump performance when working in ground mode and also to simulate a system where anti-freeze is not used.

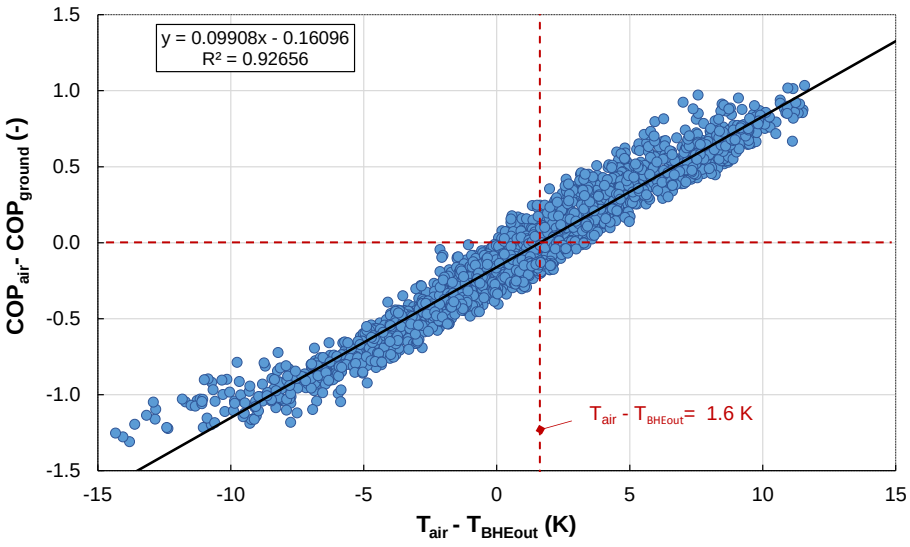

Figure 12 Difference between the hourly performance coefficients of the DSHP operating with air and ground source only against the temperature difference between the two sources ($T_{air} - T_{BHEout}$).

In the following, the results obtained with the simulation of the system working in dual-source configuration with the above-mentioned control logic (Figure 12) are reported. Figure 13 reports the evolution of the temperature of the water returning from the ground BHEs (T_{BHEout}) as simple moving average with 24 hours period during 3 years of operation. The simulation has been realized considering a time step equal to 4 h. It can be observed that after the first year, where the initial ground conditions were set starting from experimental data, the water temperature coming from the BHEs is slightly decreased but tends to follow a stable pattern without a further long-term change. The graph also reports the same result referred to the yearly simulations realized with a time step equal to 1 h for the GSHP mode only and for the DSHP operating with the same logic. It can be observed that the results obtained with the DSHP mode and different time steps (1 h for the 1-year simulation and 4 h for the three-years simulation) did not lead to remarkable variations in the temperature trends. On the contrary, if comparing the DSHP and GSHP mode, it can be observed that during the heating season the trends of the water temperature returning from the ground are substantially different. Indeed, when considering the operation of the DSHP, the variation of the ground temperature during the heating season is less sharp compared to the case of the GSHP (see Figure 13 from 5000 h to 6500 h and from 1400 h to 2500 h). In addition, Figure 14 displays the average, minimum and maximum values of $T_{DSHPout}$ obtained for the GSHP and DSHP configurations. The average water temperature obtained by the DSHP simulation results to be higher compared to the one obtained by the GSHP simulation, due to the use of the air source in the mid-season periods, reducing the use of the ground source. The operation strategy assures a temperature of the water returning from the BHEs equal to 9.9 °C during the DSHP simulation, which is more than 3 K higher than the value obtained during the GSHP simulation (equal to 6.7 °C).

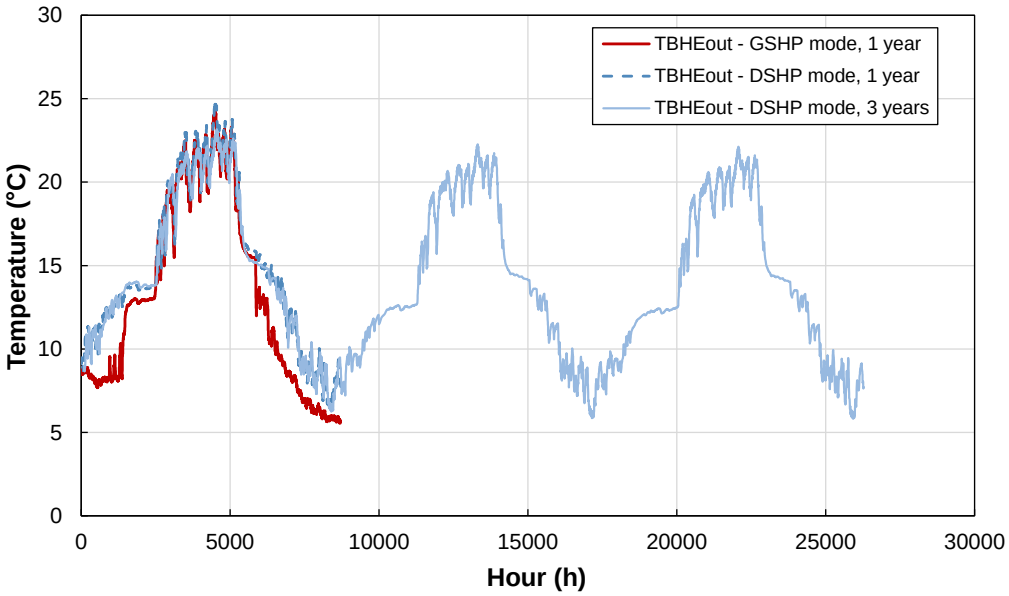

Figure 13 Temperature of the water returning from the ground (T_{BHEout}) during the three years simulation with the DSHP system (4 h time step, blue straight line), yearly simulation with the DSHP system (1 h time step, blue dotted line), yearly simulation with the GSHP system (1 h time step, red straight line). The results are reported as simple moving average with 24 hours period.

Figure 15 reports a comparison between the results of the 1-year simulations realized considering the heat pump operating with only one source/sink (as ASHP or as GSHP) and as a DSHP. Figure 15a shows the seasonal performance factor calculated according to Eq. (7) for the heating season. It has been found that the minimum SPF is obtained with the ASHP and is equal to 3.88 while the SPF is 9.8% higher in the case of GSHP operations (SPF=4.26). The SPF in the case of DSHP is equal to 4.42, thus 13.8% higher than in the case of ASHP and 3.8% higher than in the case of GSHP. This difference is due to the fact that, as suggested by Figure 13 and Figure 14, the temperature of the ground in the DSHP configuration is higher than in the ground-only operation and that the air source is used when its performance is higher. Furthermore, it was found that the ground source is used for 56% of the heating season in the DSHP configuration, whereas the air source is used for 44% of the same period (i.e. when Eq. (8) is satisfied). Two further observations can be done regarding the dual-source operation:

- During the heating period, the mean air temperature is equal to 7.6 °C, whereas the average temperature when only the air source is used (DSHP in air mode) is equal to 12 °C. This means that another advantage of this approach is the possible reduction of the defrosting cycles.
- Regarding the ground source, even if it has been mainly used during the coldest period of the heating season, the mean value of COP (equal to 3.88) was found to be 4.8% higher than in the case of the ground-only (GSHP)

operation, meaning that with the DSHP system the ground was less stressed during the coldest season and this is fundamental to preserve the ground thermal source in a long-term perspective.

In addition, the DSHP system avoids the system to reach water temperature returning from the BHE lower than 4 °C, which was not possible when working as GSHP.

Finally, Figure 15b shows the seasonal performance factor calculated according to Eq. (7) for the yearly operation: in this case, the advantage of the usage of the ground source is more prominent: compared to the ASHP (SPF=3.99), the SPF is 24.8% higher in the case of GSHP operations (SPF=4.98) and 27.9% higher in the case of DSHP operations (SPF=5.1). Therefore, the use of DSHP is even more advantageous than GSHP only, with 2.4% increase of the SPF.

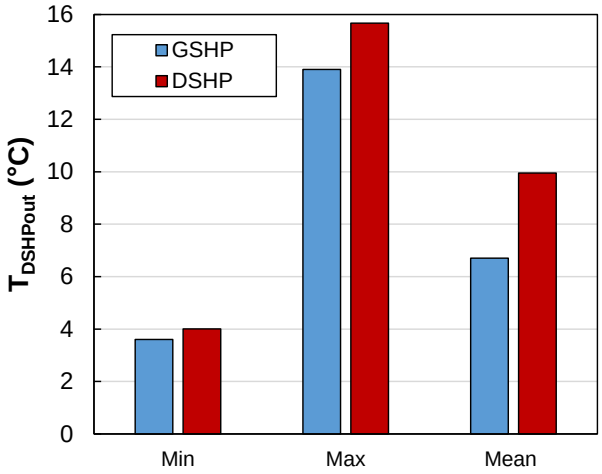

Figure 14 Calculated values of the minimum, maximum and mean water temperature at the outlet of the BHEs (T_{BHEout}) during the heating season in the case of ground-only mode (GSHP) and dual source mode (DSHP).

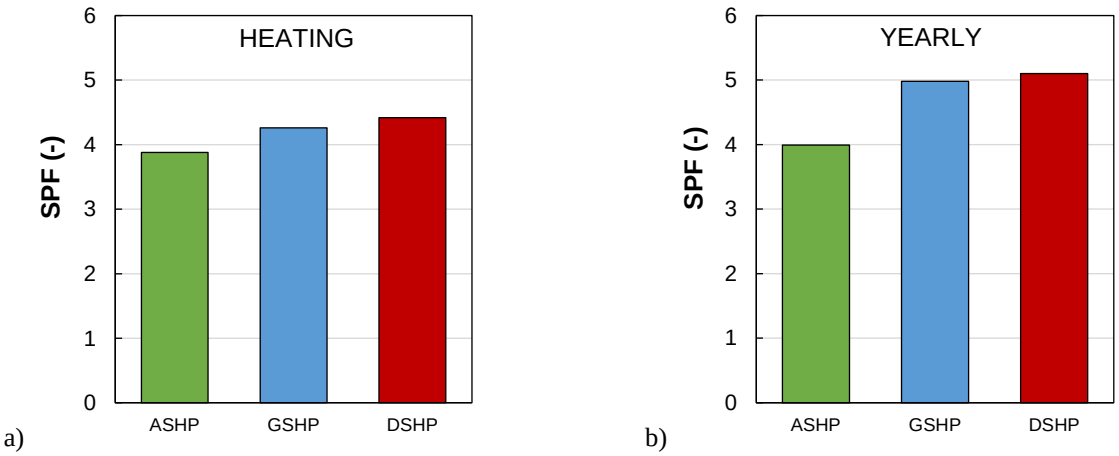

Figure 15 Seasonal performance factor obtained in the air-only mode (ASHP), ground-only mode (GSHP) and dual source mode (DSHP) during the heating season (a) and during the yearly operation (b).

5. CONCLUSIONS

In this study, a new sequential coupled model used to simulate the dynamic behaviour of a heat pump system linked to a borehole heat exchangers' field is presented. To perform the coupled simulations, an external controller has been developed in Matlab® to run consecutively two models:

- the heat pump model, which considers the physical equations that govern the heat transfer in the heat exchangers of the heat pump;
- the model of the borehole heat exchangers' field, developed using the software FEFLOW® which can operate fully transient simulations.

The coupled model can simulate several system configurations and the operations of the heat pump as an ASHP, GSHP or DSHP. The results have been compared with the experimental data obtained from the monitoring of a DSHP installed in Tribano (Italy). The analysis showed that in the winter and summer operation the average deviation between the measured and simulated water temperature entering/exiting the BHEs is below 1 K.

The validated coupled model has been used for several simulations and the main results are the followings:

- Yearly simulations of the heat pump working as an ASHP or as a GSHP have been performed. According to the simulation results: during the cooling season the GSHP can reach a SPF equal to 7.75 while the ASHP can reach a SPF equal to 4.2; during the heating season the advantage in the use of a ground source heat pump persists but reduces and the SPF is 9.8% higher compared to that of the ASHP.
- The coupled simulations highlight that when the heat pump operates entirely as a GSHP during the winter season, the heating demand is satisfied but the temperature of the water in the BHEs reaches values lower than the antifreeze limit equal to 4 °C, meaning that the borehole heat exchangers' field designed would be insufficient.
- The results of the simulations in air-only mode and ground-only mode have been used to develop a switching strategy for the heating season. In the present case, the COP operating in air mode is higher than that operating in ground mode when the temperature of the air is on average 1.6 K higher than the temperature of the water returning from the ground.
- The switching strategy between the two sources has been implemented in the controller to drive the yearly simulation of the DSHP. Considering this switching strategy, during the heating season the heat pump works with the air source for 44% of the time and the seasonal performance coefficient increases by 13.8% as compared to the air mode-only simulation and by 3.8% compared to the ground-only simulation. The

simulation proved that the addition of the air source allowed to satisfy the total energy needs, without any addition of borehole numbers or higher depth, thus with substantial investment cost savings. On the other hand, the switching strategy based on source temperature allowed to choose the best source in terms of performance, avoiding the defrost cycle in air mode and allowing a faster thermal recharge of the ground.

Finally, this paper demonstrated a new procedure to perform coupled simulations of shallow geothermal systems linked to dual-source heat pumps. Further studies will focus on the generalization of the procedure. Specifically, new simulations will be performed over different and more complex types of heat pump systems and borehole heat exchangers, with the aim to expand the number of potential applicants and end-users.

ACKNOWLEDGEMENTS

The research was supported also by the research project GEOTeCH [17], co-funded by the European Community Horizon 2020 Program for European Research and Technological Development (2014–2020) – Grant Agreement 656889. The support of Hiref S.p.A. is also acknowledged.

NOMENCLATURE

A	Area	[m^2]
ASHP	Air-source heat pump	
BP-HE	Brazed plate heat exchanger	
CB-HE, BHE	Coaxial borehole/borehole heat exchanger	
COP	Coefficient of performance	[-]
DSHP	Dual-source heat pump	
EER	Energy efficiency ratio	[-]
FC-HE	Finned coil heat exchanger	
GSHP	Ground-source heat pump	
$GWP_{100years}$	Global Warming Potential over 100 years	
HTC	Heat transfer coefficient	[W m^{-2} K^{-1}]
$\dot{m}$	Mass flow rate	[kg s^{-1}]
N	Total number of time steps	[-]
NTU	Number of Transfer Units	[-]
OB	Observation Borehole	
P	Heat pump consumption	[W]
Q	Heat flow rate, heating/cooling capacity	[W]
R	Thermal resistance	[m^2 K W^{-1}]
SC	Subcooling	[K]
SH	Superheating	[K]
SPF	Seasonal performance factor	[-]
T	Temperature	[°C]
Tol	Tolerance value for convergence	[K]
U	Global heat transfer coefficient	[W m^{-2} K^{-1}]
Δt	Time step	[s]

ΔT_{lim}	Limit temperature difference	[K]
ΔT_{ml}	Logarithmic mean temperature difference	[K]

Subscripts

air, AIR	Air
BHE	Borehole heat exchanger side
BP	Brazed plate
C	Condenser, water side
Cd	Conduction
Cond	Condenser
D	Difference
E	Evaporator, water side
Evap	Evaporator
GUESS	Guess/initial value
I	Heat exchanger discretization
In	Inlet
J	BP-HE discretization
Lim	Limit
Max	Maximum
Meas	Measured
n	Time step
N	Total number of time steps
NEW	New/updated value
Out	Outlet
R	Refrigerant
Re	BP-HE region
Sim	Simulated
USER	User side

Greek symbols

E	FC-HE effectiveness	[-]
η_{comp}	Compressor efficiency	[-]

REFERENCES

1. Kavanaugh, S.P.; Rafferty, K. Design of geothermal systems for commercial and institutional buildings. *ASHRAE Trans.* **1997**.
2. Focaccia, S.; Tinti, F.; Monti, F.; Amidei, S.; Bruno, R. Shallow geothermal energy for industrial applications: A case study. *Sustain. Energy Technol. Assessments* **2016**.
3. Cui, Y.; Zhu, J.; Twaha, S.; Riffat, S. A comprehensive review on 2D and 3D models of vertical ground heat exchangers. *Renew. Sustain. Energy Rev.* 2018.
4. Al-Khoury, R.; Kölbel, T.; Schramedei, R. Efficient numerical modeling of borehole heat exchangers. *Comput. Geosci.* **2010**.
5. Javed, S.; Claesson, J. New analytical and numerical solutions for the short-term analysis of vertical ground heat exchangers. In Proceedings of the ASHRAE Transactions; 2011.
6. Pasquier, P.; Marcotte, D. Short-term simulation of ground heat exchanger with an improved TRCM. *Renew. Energy* **2012**.
7. Ruiz-Calvo, F.; De Rosa, M.; Acuña, J.; Corberán, J.M.; Montagud, C. Experimental validation of a short-term Borehole-to-Ground (B2G) dynamic model. *Appl. Energy* **2015**.
8. Li, X.; Lyu, W.; Ran, S.; Wang, B.; Wu, W.; Yang, Z.; Jiang, S.; Cui, M.; Song, P.; You, T.; et al. Combination principle of hybrid sources and three typical types of hybrid source heat pumps for year-round efficient operation. *Energy*

2020, *193*.
9. Grossi, I.; Dongellini, M.; Piazzi, A.; Morini, G.L. Dynamic modelling and energy performance analysis of an innovative dual-source heat pump system. *Appl. Therm. Eng.* **2018**, *142*, 745–759.
10. Lazzarin, R.; Noro, M. Photovoltaic/Thermal (PV/T)/ground dual source heat pump: Optimum energy and economic sizing based on performance analysis. *Energy Build.* **2020**.
11. De Rosa, M.; Ruiz-Calvo, F.; Corberán, J.M.; Montagud, C.; Tagliafico, L.A. A novel TRNSYS type for short-term borehole heat exchanger simulation: B2G model. *Energy Convers. Manag.* **2015**.
12. Hein, P.; Kolditz, O.; Görke, U.J.; Bucher, A.; Shao, H. A numerical study on the sustainability and efficiency of borehole heat exchanger coupled ground source heat pump systems. *Appl. Therm. Eng.* **2016**.
13. Li, C.; Mao, J.; Zhang, H.; Xing, Z.; Li, Y.; Zhou, J. Numerical simulation of horizontal spiral-coil ground source heat pump system: Sensitivity analysis and operation characteristics. *Appl. Therm. Eng.* **2017**.
14. Corberán, J.M.; Cazorla-Marín, A.; Marchante-Avellaneda, J.; Montagud, C. Dual source heat pump, a high efficiency and cost-effective alternative for heating, cooling and DHW production. *Int. J. Low-Carbon Technol.* **2018**, *13*, 161–176.
15. Diersch, H.J.G.; Bauer, D.; Heidemann, W.; Rühaak, W.; Schätzl, P. Finite element modeling of borehole heat exchanger systems. Part 2. Numerical simulation. *Comput. Geosci.* **2011**.
16. Zanetti, E.; Azzolin, M.; Bortolin, S.; Busato, G.; Del Col, D. Experimental data and modelling of a dual source reversible heat pump equipped with a minichannels evaporator. *Therm. Sci. Eng. Prog.* **2022**.
17. GEOTECH - Geothermal Technology for €conomic Cooling and Heating. Available online: https://cordis.europa.eu/project/id/656889.
18. IPCC *Climate Change 2014: Synthesis Report. Contribution of Working Groups I, II and III to the Fifth Assessment Report of the Intergovernmental Panel on Climate Change*; 2014; ISBN 9789291691432.
19. Tinti, F.; Carri, A.; Kasmaee, S.; Valletta, A.; Segalini, A.; Bonduà, S.; Bortolotti, V. Ground temperature monitoring for a coaxial geothermal heat exchangers field: Practical aspects and main issues from the first year of measurements. *Rud. Geol. Naft. Zb.* **2018**.
20. Rich, D.G. Effect of Fin Spacing on the Heat Transfer and Friction Performance of Multi-Row, Smooth Plate Fin-and-Tube Heat Exchangers. *ASHRAE Trans.* **1973**, *79*, 137–145.
21. Pichtel, J. *Handbook of Chemical and Environmental Engineering Calculations*; 2003; Vol. 32; ISBN 0071433260.
22. Cavallini, A.; Del Col, D.; Doretti, L.; Matkovic, M.; Rossetto, L.; Zilio, C.; Censi, G. Condensation in horizontal smooth tubes: A new heat transfer model for heat exchanger design. In Proceedings of the Heat Transfer Engineering; 2006; Vol. 27, pp. 31–38.
23. Azzolin, M.; Berto, A.; Bortolin, S.; Del Col, D. Condensation heat transfer of R1234ze(E) and its A1 mixtures in small diameter channels | Transfert de chaleur par condensation du R1234ze(E) et de ses mélanges A1 dans des canaux de faible diamètre. *Int. J. Refrig.* **2022**, *137*, 153–165.
24. Azzolin, M.; Bortolin, S. Condensation and flow boiling heat transfer of a HFO/HFC binary mixture inside a minichannel. *Int. J. Therm. Sci.* **2021**.
25. Matkovic, M.; Cavallini, A.; Del Col, D.; Rossetto, L. Experimental study on condensation heat transfer inside a single circular minichannel. *Int. J. Heat Mass Transf.* **2009**, *52*, 2311–2323.
26. Liu, Z.; Winterton, R.H.S. A general correlation for saturated and subcooled flow boiling in tubes and annuli, based on a nucleate pool boiling equation. *Int. J. Heat Mass Transf.* **1991**, *34*, 2759–2766.
27. Webb, R.L. Convective condensation of superheated vapor. *J. Heat Transfer* **1998**, *120*, 418–421.
28. Martin, H. A theoretical approach to predict the performance of chevron-type plate heat exchangers. *Chem. Eng. Process. Process Intensif.* **1996**, *35*, 301–310.
29. Longo, G.A.; Righetti, G.; Zilio, C. A new computational procedure for refrigerant condensation inside herringbone-type Brazed Plate Heat Exchangers. *Int. J. Heat Mass Transf.* **2015**, *82*, 530–536.
30. Amalfi, R.L.; Vakili-Farahani, F.; Thome, J.R. Flow boiling and frictional pressure gradients in plate heat exchangers. Part 2: Comparison of literature methods to database and new prediction methods. *Int. J. Refrig.* **2016**, *61*, 185–203.
31. EN-12900:2013. Refrigerant compressors. Rating conditions, tolerances and presentation of manufacturer's performance data. **2013**.
32. Al-Khoury, R.; Bonnier, P.G.; Brinkgreve, R.B.J. Efficient finite element formulation for geothermal heating systems. Part I: Steady state. *Int. J. Numer. Methods Eng.* **2005**.
33. Al-Khoury, R.; Bonnier, P.G. Efficient finite element formulation for geothermal heating systems. Part II: Transient. *Int. J. Numer. Methods Eng.* **2006**.
34. Tinti, F.; Azzolin, M.; Bonduà, S.; Zanetti, E.; Bortolin, S.; Busato, G.; Focaccia, S.; Marín, A.C.; Bortolotti, V. Sequential coupled simulation of a dual source heat pump and shallow geothermal reservoir. In Proceedings of the European Geothermal Congress; 2019; pp. 11–14.
35. Nam, Y.; Ooka, R.; Hwang, S. Development of a numerical model to predict heat exchange rates for a ground-

source heat pump system. *Energy Build.* **2008**.
36. Rivera, J.A.; Blum, P.; Bayer, P. Analytical simulation of groundwater flow and land surface effects on thermal plumes of borehole heat exchangers. *Appl. Energy* **2015**.
37. Nam, Y.; Ooka, R. Numerical simulation of ground heat and water transfer for groundwater heat pump system based on real-scale experiment. *Energy Build.* **2010**.
38. Cazorla-Marín, A.; Montagud-Montalvá, C.; Tinti, F.; Corberán, J.M. A novel TRNSYS type of a coaxial borehole heat exchanger for both short and mid term simulations: B2G model. *Appl. Therm. Eng.* **2020**.
39. ARPAV Agenzia Regionale per la Prevenzione e Protezione Ambientale del Veneto. Available online: https://www.arpa.veneto.it/.
40. Azzolin, M.; Cattelan, G.; Dugaria, S.; Minetto, S.; Calabrese, L.; Del Col, D. Integrated CO2 systems for supermarkets: Field measurements and assessment for alternative solutions in hot climate. *Appl. Therm. Eng.* **2021**.

Reviewer #1: This paper proposed a numerical model to calculate the performance of a dual-source (air source and ground source) heat pump, and used tested data from an actual project to validate the model. Then, the model was used to calculate the performance of a dual-source system and determine its operating strategy.

The questions asked by the reviewer have been well answered, and the recommendations have been reflected in the revised manuscript. Thereby, the manuscript can be accepted after being carefully checked. For example, in answer to the 8th comment from Reviewer 1, the following sentence needs commas: "To verify the accuracy of the LUTs the results obtained with the DSHP model using the look-up tables have been compared with the results obtained with the DSHP model at some conditions that have not been used for LUT construction and reported in Table 3".

We thank the Reviewer for the comment.

The manuscript has been checked carefully and the typos have been corrected.

Reviewer #2: A numerical model of air/ground-source heat pump is developed in MATLAB, and it validity is verified with experimental data from a shallow geothermal plant. By this numerical model, the system performance, long-term production and the sustainability of the geothermal reservoir are evaluated. Then, the switching control strategy of dual-sources heat pump is determined and a better performance is achieved compared to the conversional air source heat pump. Before being published, the several details need to be adjusted. Some questions and suggestions are as follows:

(1) The layout of dual-source heat pump (Figure 1) is suggested to be drawn in more detailed, such as the relationship of target building and evaporator/condenser, the relationship of ground and air sources under different operating condition.

The layout of the heat pump in Figure 1 has been further clarified as suggested by the reviewer.
In the new version of Figure 1, the connections in the secondary loops/heat exchangers have been better detailed. The new Figure is reported below.

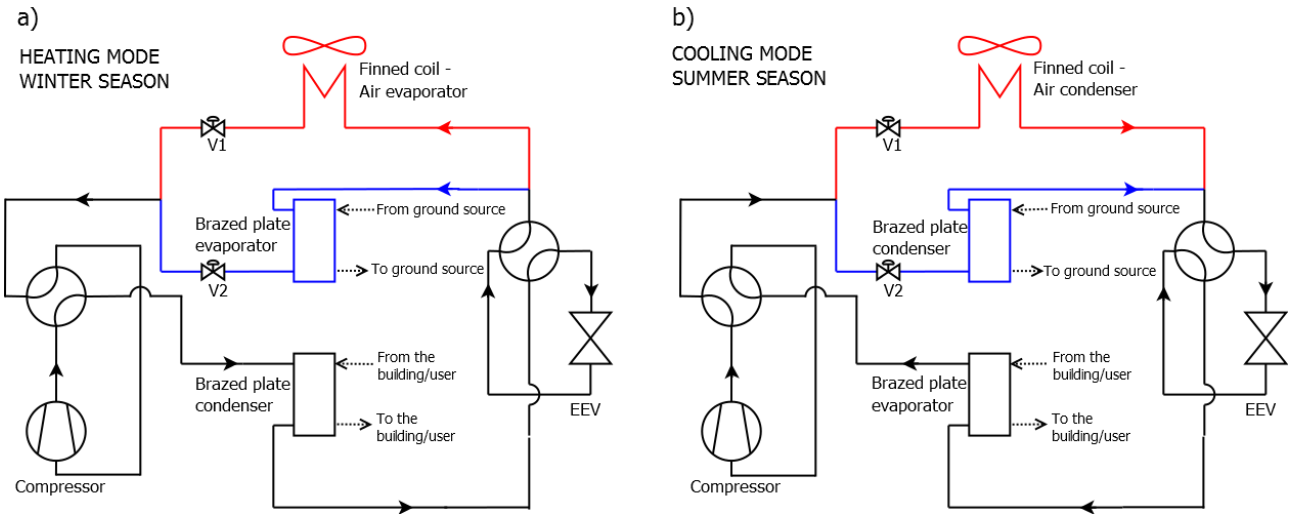

(2) It is claimed in the first sentence of Section 2.1 that the dual-source heat pump can provide the domestic hot water. However, the hot water (about 50℃) is not mentioned again in the following text.

The present study considers a real heat pump prototype installed in an office building in Tribano, located in the alluvial Po Plain (45°12’ 32’’ N 11°50’ 44’’ E) in Italy. The heat pump prototype has been designed and constructed to satisfy all the thermal needs: heating, cooling and sanitary hot water. However, in the present study, we discussed the usage of the system to produce chilled and hot water to satisfy the cooling and heating demand of the user. Therefore, following the reviewer’s comment, this has been clarified in the manuscript.

Section 2.1. *“The prototype heat pump used in this study has been designed for residential applications or small offices: it has a nominal heating capacity equal to 16 kW and it can provide chilled and hot water to satisfy the building’s thermal demands”*

Section 3.1. “*The DSHP started working in November 2017 and, after a testing period, it became fully operational in summer 2018 providing heating and cooling to the building*”

(**3) Is it necessary to display the yearly simulation/analysis results of ASHP and GSHP in Section 4.1?**

The yearly simulations realized when the heat pump operates as an ASHP and as a GSHP have been presented and discussed since they represent the starting point for the development of the switching strategy between the thermal sources. Indeed, the results presented in Section 4.1, have been used to define the switching parameter and the control strategy presented in Section 4.2. In addition, yearly simulations allow understanding that, during the cooling period, the performance of the prototype working in ground mode-only is higher compared to the air mode-only operation; while considering the heating period the use of this undersized CB-HE field is not always convenient, leading to low water temperatures inside the BHEs. For these reasons, we prefer to display the yearly simulation results in Section 4.1.

(4) It is suggested to demonstrate the comparison of ASHP during the heating season in Figure 14.

The comparison, requested by the Reviewer, between ASHP, GSHP and DSHP is presented in Figure 15a. Figure 14 displays the temperatures of the water returning from the boreholes. These temperatures have been calculated using the coupled numerical model. In Figure 14, the temperature of the air could be reported but the air temperature is an input to the model and not a result. In addition, the results in Figure 14 demonstrate that, when a DSHP is used, the ground can be less stressed during the winter season compared to the standard work of a GSHP.

To clarify this, the text anticipating Figure 14 in the Section 4.2 of the manuscript has been changed as follows:

"In addition, Figure 14 displays the average, minimum and maximum values of T_DSHPout obtained for the GSHP and DSHP configurations. The average water temperature obtained by the DSHP simulation results to be higher compared to the one obtained by the GSHP simulation, due to the use of the air source in the mid-season periods, reducing the use of the ground source. The operation strategy assures a temperature of the water returning from the BHEs equal to 9.9 °C during the DSHP simulation, which is more than 3 K higher than the value obtained during the GSHP simulation (equal to 6.7 °C)."

(5) If the definition of COP is presented in the text, it will help to understand the content of the paper.

According to the Reviewer's comment, the definition of the performance coefficient is now presented in the text (Section 3.3, new equation 6):

"The results of this comparison are reported in Figure 10 in terms of cooling/heating capacity and performance coefficients (EER, COP), which are calculated as the ratio between the cooling/heating capacity Q and the heat pump power consumption P:

$$EER\ ,COP = \frac{Q}{P} \qquad \textit{Eq. (1)}$$

The subsequent equations have been renumbered accordingly.

Sequential coupled numerical simulations of an air/ground-source heat pump: validation of the model and results of yearly simulations

ZANETTI Emanuele[1], BONDUÀ Stefano[2], BORTOLIN Stefano[1], BORTOLOTTI William[2], AZZOLIN[1]* Marco, TINTI Francesco[2]

[1] Department of Industrial Engineering, University of Padova, Via Venezia 1, 35131 - Padova, Italy

[2] Department of Civil, Chemical, Environmental, and Materials Engineering, University of Bologna, Via Terracini 28, 40131 – Bologna Italy

ABSTRACT

Numerical simulations are important tools for the assessment of exploiting geothermal energy in heat pump applications. They can be used to evaluate the performance of the system, the long-term production scenarios and the sustainability of the geothermal reservoir. The present work introduces and describes a numerical model, in which a dedicated Matlab® script has been realized to allow sequentially coupled simulations of a shallow geothermal reservoir and of a heat pump system. A mathematical model of a dual-source heat pump, working alternatively with the ground or the air as heat source/sink, has been developed in Matlab® environment. The heat exchangers of the heat pump have been modelled considering the equations that govern the physical phenomena. The dynamic numerical simulator FEFLOW®, based on the finite element method, has been used to simulate the behaviour of the geothermal reservoir, subjected to heat extraction/reinjection by a closed loop vertical heat exchangers field. This methodological approach is useful to evaluate the performance of the coupled system in the long term, and it is important for understanding the advantages and limits of the dual-source heat pump in assuring sustainability over time avoiding the depletion of geothermal resources. The models and their coupling have been calibrated and validated with experimental data from a shallow geothermal plant located in Tribano (Padova, IT). It consists of eight coaxial borehole heat exchangers 30 m deep, connected to a 16 kW dual-source heat pump prototype. The heat pump system provides heating and cooling to an office area. The coupled model has been used to compare the performance of the heat pump when working in air-mode only or in ground-mode only. This allowed the development of a switching control strategy between the two thermal sources. Yearly simulations with the switching strategy have shown that the seasonal performance factor of the dual-source heat pump during the heating mode can be 13.8% higher compared to the one obtained with a conventional air source heat pump and 3.8% higher with respect to a ground source heat pump.

1. INTRODUCTION

Dual-source heat pumps (DSHPs) can work alternatively with air or ground as heat source/sink and nowadays are seen as an interesting solution because they allow the reduction of the length of the borehole heat exchangers and thus the investment costs. When a DSHP exchanges heat with ambient air, it works as an air-source heat pump (ASHP). On the contrary, when it uses the ground as source/sink it operates as a ground source heat pump (GSHP) following a sequential logic: the heat pump, depending on the building loads, requests an energy amount from the geothermal probes, which exchange heat with the thermal reservoir (Kavanaugh and Rafferty [1]). This process can cause both short and long-term thermal depletion of the reservoir, which must be predicted and managed, to allow the optimal operation of the GSHP system (Focaccia et al. [2]). Numerical simulation is a standard approach in GSHP projects to study the short and long-term thermal depletion of the ground. Indeed, the ultimate purpose is to obtain information to improve and optimize the behaviour over time of the system to increase its efficiency and consequently obtain energy savings (Cui et al. [3]). Many software packages exist to numerically simulate the behaviour of the ground subjected to heat extraction/injection cycles. Some notable case studies of this approach can be found in Al-Khoury et al. [4], Javed and Claesson [5], Pasquier and Marcotte [6], Ruiz-Calvo et al. [7]. The above-mentioned studies focus on the model of the thermal reservoir while they adopt a simplification for the heat pump, which is not modelled and the thermal load exchanged which is defined as a hypothesis. On the other side, there are various models of ground source or dual-source heat pump systems (Li et al. [8], 193, Grossi et al. [9], Lazzarin and Noro [10]) and the TRNSYS simulation tool is widely used [11]. This approach is useful when the main goal is to study the performance of a specific heat pump coupled with a building and its heating distribution system. Often these models rely on the manufacturer's data to determine the behaviour of the heat pump (Hein et al. [12], Li et al. [13]) or on correlations obtained with experimental measurements conducted on the specific heat pump (Corberan et al. [14]). The main drawback of these approaches is that they do not consider the physical phenomena occurring in the heat exchangers and thus they can be applied with difficulty when considering a different refrigerant or different heat exchangers.

It emerges that in the literature there is a lack of works dealing with the modelling of DSHPs that are able to simulate the ground thermal reservoir and the heat pump. The present paper is aimed to cover this gap and presents a new modelling approach that considers the coupling between the numerical model of a shallow geothermal reservoir and the numerical model of a dual-source heat pump. The type of coupling between the two simulators is "sequential", which means that the connection between the two simulators takes place through data files generated by the simulators themselves and managed by a control program. That is, each simulator generates an output data file that is used as

input file for the other simulator in a continuous cycle supervised by an external software layer controlling the correct execution of the coupled simulation and determining its beginning and end. Moreover, the model of the shallow geothermal reservoir is realized with the Finite Element Modeling software package FEFLOW® which is among the most precise and used tools in shallow geothermal design (Diersch [15]) and the model of the heat pump considers the physical equations governing the heat transfer phenomena [16].

The coupled simulator has been calibrated and validated with the experimental data of an existing DSHP with eight geothermal probes installed in Tribano (Padova, Italy) in the framework of the European Project GEOTeCH [17], (see Section 3). Then the coupled simulator has been used to perform yearly simulations of the functioning of the DSHP considering optimum switching strategies between the thermal sources (see Section 4).

2. HEAT PUMP-GEOTHERMAL SHALLOW SEQUENTIALLY COUPLED SIMULATOR

In this Section, the dual source heat pump prototype and the borehole heat exchangers' field are presented. The numerical coupled simulator (DSHP-BHE controller) composed by the combination of the heat pump model and of the shallow reservoir model is described in detail.

2.1 Dual-source heat pump prototype

The prototype heat pump used in this study has been designed for residential applications or small offices: it has a nominal heating capacity equal to 16 kW and it can provide chilled and hot water to satisfy the building's thermal demands. The heat pump is dual source, thus it can work with air or ground as thermal source/sink to absorb or reject heat through a water-to-refrigerant or an air-to-refrigerant heat exchanger. The working refrigerant is R32 (hydro-fluorocarbon refrigerant with $GWP_{100years}$ equal to 677 [18]), which has a global warming potential three times lower than that of R410A commonly used in these applications. The layout of the heat pump is reported in Figure 1. The heat pump is equipped with an inverter-driven scroll compressor that allows to follow the thermal load requested by the user. When the heat pump operates in heating mode (Figure 1a), after the compressor, the refrigerant enters the condenser, which is a brazed plate heat exchanger (BP-HE) and it heats the water of the building distribution system. After the condenser, the refrigerant passes through the electronic expansion valve (EEV) and it evaporates in the finned coil heat exchanger (when using air as thermal source) or in the brazed plate heat exchanger (when using the water from the borehole heat exchanger field as thermal source). When the heat pump operates in cooling mode (Figure 1b),

after the compressor, the refrigerant is condensed in the finned coil heat exchanger (when using air as thermal sink) or in the brazed plate heat exchanger (when using the water from the borehole heat exchanger field as thermal sink). After the condenser, the refrigerant passes through the electronic expansion valve and then produces chilled water in the user brazed plate evaporator. Detailed information regarding the heat pump prototype can be found in [16].

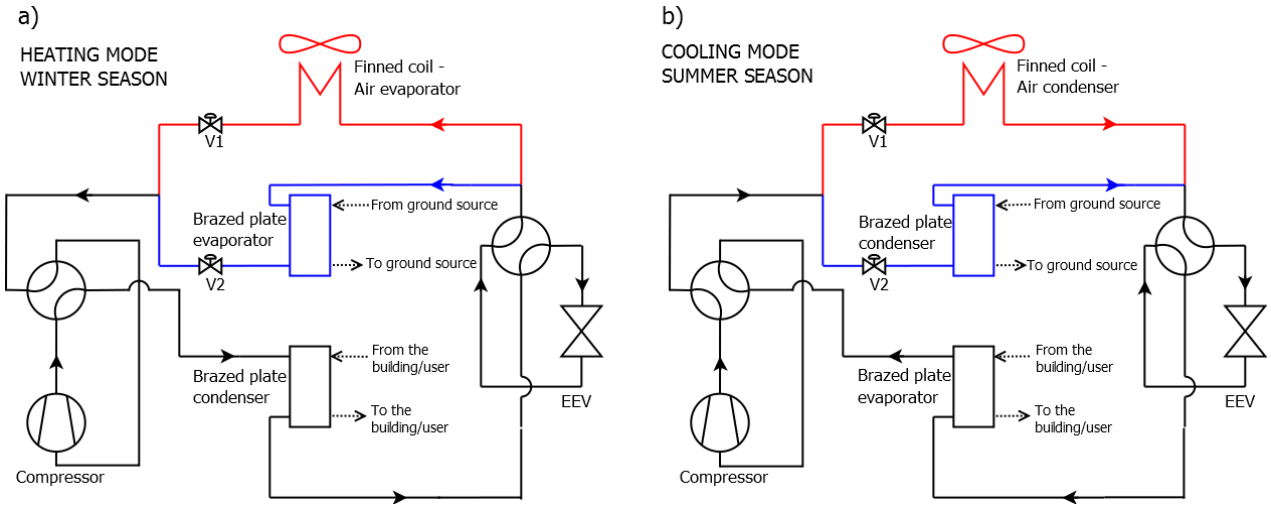

Figure 1 Layout of the dual-source heat pump. a) Refrigerant loop when operating in heating mode (winter season), b) refrigerant loop when operating in cooling mode (summer season). The black solid lines represent the main path of the refrigerant loop, the red solid lines represent the path when using the air source and the blue solid lines represent the path when using the ground source. The solenoid valves V1 and V2 manage to change between the operative modes. EEV is the electronic expansion valve.

2.2 Borehole heat exchangers' field

The borehole heat exchangers' field used for this study includes eight coaxial probes (coaxial borehole heat exchanger - CB-HE), spaced 6 m, down to 30 m deep, without grouting, the latter allowed by local environmental authority of the study area. The shallowest layers are formed by unconsolidated, alluvial soils, with very fine grain size – silt and clay – of low permeability, locally interspersed by sandy layers. The eight CB-HEs are connected in parallel to a central collector and subsequently to the DSHP. The working fluid is pure water. The main parameters of each CB-HE installed are reported in *Table 1*. Besides the eight CB-HEs, three Observation Boreholes (OBs) have been installed to monitor the ground temperature. Further details of the geology and hydrogeology of the area, the monitoring strategy and the system layout can be found in Tinti et al.[19].

Borehole diameter (m)	Inlet Pipe Diameter (m)	Inlet Pipe Wall Thickness (m)	Inlet Pipe Thermal Conductivity (W/(m·K))	Outlet Pipe Diameter (m)	Outlet Pipe Wall Thickness (m)	Outlet Pipe Thermal Conductivity (W/(m·K))
0.15	0.09	0.0029	0.42	0.06	0.0029	0.42

Table 1 Data of each coaxial borehole heat exchanger connected to the DSHP used for the study.

2.3 Heat pump numerical model

The numerical model of the heat pump (named DSHP model) has been developed in Matlab® environment and it considers all the components of the heat pump to simulate its operation during steady-state conditions. In particular, the models of the heat exchangers have been developed considering a finite discretization over their volume and each discretized element as an independent heat exchanger where continuity, momentum and energy equations are solved. This approach allows the model to be flexible and to estimate the performance of heat pumps operating also with various heat exchanger geometries and refrigerants.

When considering the model of the finned coil heat exchanger (FC-HE), its volume is subdivided into identical elements which are sequentially treated following the refrigerant path. For each $i-th$ element, the refrigerant outlet condition is calculated based on the ε-NTU method. The effectiveness of the heat exchanger is defined as:

$$\varepsilon_i = Q_i / Q_{max,i} \qquad \text{Eq. (1)}$$

where Q_i is the heat flow rate exchanged in the tube element and $Q_{max,i}$ is the maximum heat flow rate that can be exchanged in a perfect counter-current configuration with an infinite heat transfer area. The Number of Transfer Units (NTU_i) of the tube element depends on the $(U_i A_i)$ product, where A_i is the heat transfer area and U_i is the global heat transfer coefficient:

$$U_i = \frac{1}{1/HTC_r + R_{cd} + 1/HTC_{air}} \qquad \text{Eq. (2)}$$

where HTC_r and HTC_{air} are the local heat transfer coefficients of the refrigerant and of the air and R_{cd} is the thermal conduction resistance of piping and fins.

The air-side heat transfer coefficient is calculated through the equations of Rich [20] and a modeling of the air dehumidification has also been implemented following the procedure proposed by Threlkeld [21]. On the refrigerant side, when the finned coil works as the condenser, the heat transfer coefficient has been evaluated with the Cavallini et al. [22] correlation which has been proved in various works to give good predictions even with small diameter channels and when using R32 (Azzolin et al.[23], Azzolin and Bortolin [24], Matkovic et al. [25]). When working as the evaporator, the refrigerant heat transfer coefficient is calculated with the Liu and Winterton [26] equation. The Dittus-Boelter equation for the heat transfer coefficient has been used in the zones of the heat exchanger where the refrigerant is single phase (desuperheating and subcooling regions in the condenser and superheating region in the evaporator). Finally, the approach of Webb [27] has been adopted for the condensation in superheated vapor. Once the equations for all the discretized elements have been solved using a guessed value of the evaporation/condensation temperature,

the refrigerant outlet conditions obtained by the sequential calculations are compared to the desired values of the outlet superheating/subcooling. Based on this comparison, the condensation/evaporation pressure is updated, and the process repeats until convergence.

In the model of the BP-HEs, the total volume of a representative plate of the heat exchanger is subdivided into various elements of different sizes. First, some macro-regions ($re-th$) are identified based on the refrigerant heat transfer process (desuperheating, condensation and subcooling for the BP-HE condenser; evaporation and superheating for the BP-HE evaporator). Each $re-th$ region is subdivided into discrete elements where the same amount of heat Q_{re} is transferred. Indeed, with this approach, the heat to be transferred in each element is known and this allows to calculate the $j-th$ heat transfer area (for a $j-th$ discretized element pertaining to the $re-th$ region) with the following relationship:

$$A_j = \frac{Q_{re}}{U_j \cdot \Delta T_{ml,j}} \qquad \text{Eq. (3)}$$

where A_j and U_j are the heat transfer area and the global heat transfer coefficient, respectively; $\Delta T_{ml,j}$ is the logarithmic mean temperature difference.

Regarding the BP-HE condenser, the heat transfer coefficient for the single-phase regions (refrigerant in the desuperheating and subcooling zone and also water) has been calculated with the Martin [28] correlation for single-phase, while in the condensation of saturated vapour region, the refrigerant heat transfer coefficient has been evaluated with the equation proposed by Longo et al. [29] (the Webb approach [27] is used for the condensation in the superheated region). When the BP-HE works as evaporator, the heat transfer coefficient for the single-phase regions is calculated with the Martin [28] correlation and the refrigerant heat transfer coefficient in the two-phase zone is calculated with the Amalfi et al. correlation [30].

Once the area of each element is determined, the overall heat exchanger surface is computed as a summation over all the elements and it is compared with the real BP-HE surface considering the following ratio:

$$r = \frac{\sum A_j}{A_{BP}} \qquad \text{Eq. (4)}$$

where A_{BP} is the effective BP-HE heat transfer area. The condensation/evaporation pressure is thus updated until r reaches a value close to unity.

Regarding the compressor, a specific subroutine has been developed: it includes the polynomial maps of the compressor according to the reference standard [31]. These polynomials manage to calculate the corresponding power

consumption and mass flow rate, which is an input for the heat exchangers subroutines. More information about the compressor model can be found in [16].

The schematic flow chart of the iterative algorithm of the model is displayed in Figure 2.

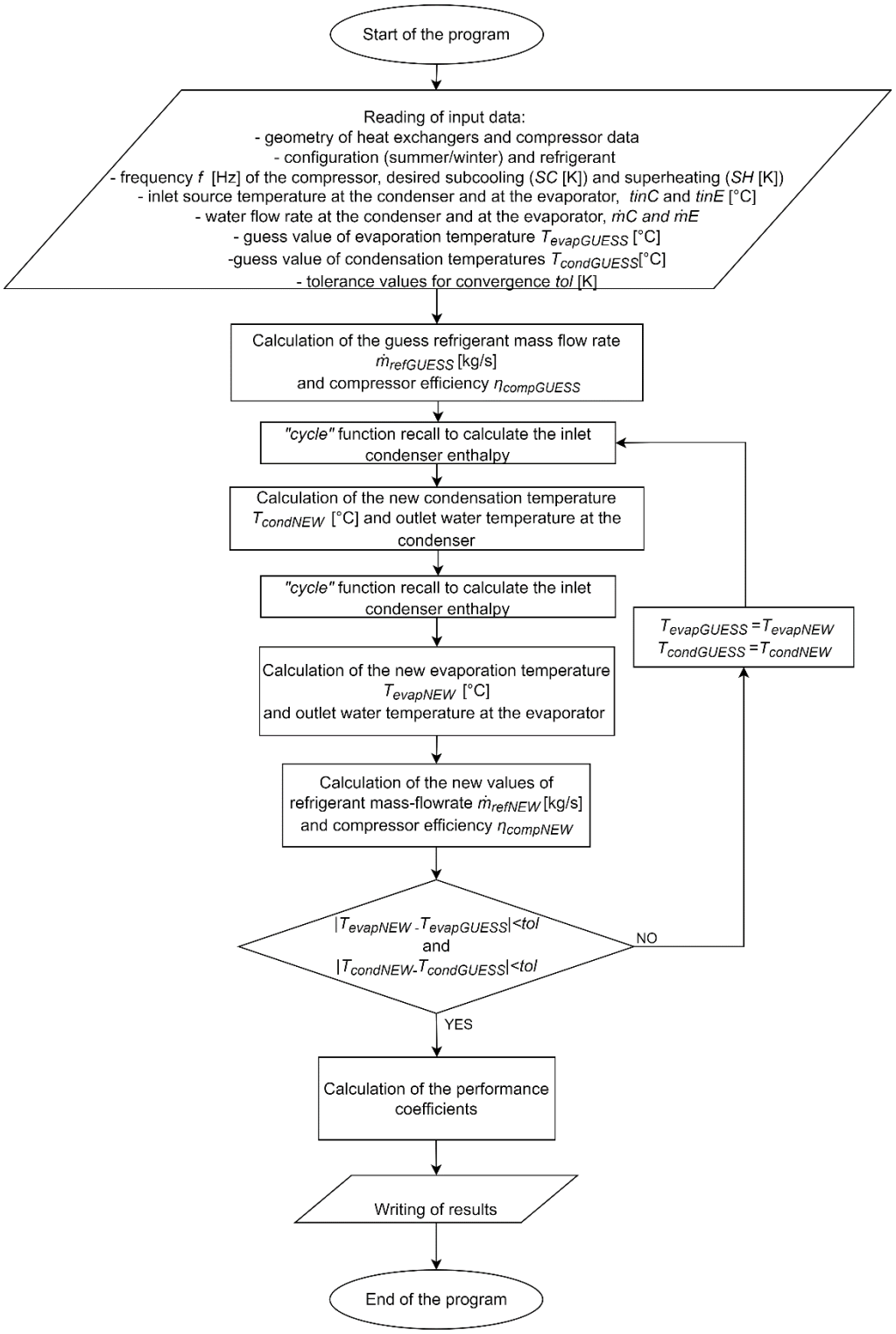

Figure 2 Flow chart of the algorithm of the DSHP model.

The required inputs of the DSHP model are: the compressor frequency (f); mass flow rate and the water temperature ($T_{USERout}$) on the user side; mass flow rate and temperatures (T_{BHEout} or T_{AIRout}) of the external source/sink (no temperature differences are assumed between T_{BHEout} and the inlet temperature at the ground brazed plate heat exchanger); the refrigerant subcooling temperature at the condenser outlet (SC); the refrigerant superheating temperature at the evaporator outlet (SH); first attempt values for the condensation and evaporation temperatures ($T_{evapGUESS}$, $T_{condGUESS}$). The algorithm starts with the calculation of first attempt values of the compressor efficiency ($\eta_{compGUESS}$) and refrigerant mass flow rate ($\dot{m}_{rGUESS}$) by means of the compressor subroutine. After determining all the initial values, an iteration cycle begins and at each iteration, new values for condensation/evaporation pressure, compressor efficiency and refrigerant mass flow rate are provided by the models described above. During the runtime, a particular subroutine called "cycle" is recalled and it is used to solve the refrigerant thermodynamic cycle, i.e. calculate the refrigerant conditions (enthalpy at the inlet-outlet of each component) based on the partial results. The entire procedure stops when the condensation/evaporation temperatures reach convergence values.

2.4 Geothermal shallow reservoir numerical model

In order to evaluate the behaviour of geothermal probes exchanging heat with the ground, a dynamic simulator is necessary. In this specific application, the software FEFLOW® (Finite Element Flow simulator) has been chosen, which has a dedicated section for modelling and simulating Borehole Heat Exchangers (BHEs) and allows the definition of the hydrogeological modelling of the studied area. The numerical model implemented is based on Al-Khoury ([32,33]) and includes specific equations for various types of BHE. A finite element formulation is derived for describing both steady and transient states of heat transfer between the BHE and the ground. The conservation of mass in groundwater flow and the continuity of energy for heat flow are included as governing differential equations for 3D systems. FEFLOW® can operate fully transient simulations and allows the realization of as many layers as needed and upload from a database of thermophysical, petrophysical and physical information for each layer (thermal conductivity, thermal capacity, hydraulic conductivity, temperature). This is important because in this application the vertical temperature gradient around the BHEs varies in time, subjected to both weather conditions and heat exchanged with the heat pump. In the specific case, the model domain implemented extends around the CB-HEs field, for a total surface area of 50 x 78 m^2 and a depth of 44 m [34]. A tetrahedral mesh was used with refinement regions around the eight CB-HEs. A set of observation points have been inserted in correspondence of the three OBs installed to monitor the undisturbed and disturbed ground temperature. A series of nine layers was used to detail the geology of the area. Layer 1 is a buffer

layer on the top, introducing the weather impact boundary condition, while Layers 2-8 cover the length of the CB-HE, 30 m, and finally Layer 9 guarantees the existence of a geothermal heat flow from the bottom. The impact of ambient weather down with depth, and its variation across seasons, was added at the borders of the model, as temperature boundary conditions, varying with depth and time. A difference in the hydraulic head from 1.5 m (top right corner) to 1.6 m (bottom left corner) takes into account the groundwater flow movement, according to the available hydrogeological information. Estimated values of ground properties, such as the hydraulic conductivity (1 m/d), the effective porosity (30%), the thermal conductivity (3 W/(m K)) and the heat capacity (2.5 MJ/(m^3·K)) have been used in the model according to the information acquired from hydrogeological studies (Tinti et al., 2018 [19]). The ground natural state is provided by simulating the thermal state of the model, without activation of the CB-HE for several years, and then validating the temperature results in the nodes corresponding to the measurement points of the three OBs. Temperature values at the nodes among the measured values and the CB-HEs are calculated by linear interpolation for each depth.

2.5 Coupled simulator: Matlab script allowing sequential coupled simulation

To simulate all the possible operative modes of the heat pump, a DSHP-BHE controller has been developed in MATLAB® to link the DSHP model and the model of the BHEs. The schematic of the system, including the common variables between the two models, is displayed in Figure 3a. The controller is able to run transient simulations of the system and its inputs are the external air temperature, the initial ground temperature distribution (which can be either natural state, or already thermally disturbed condition including the BHE field), the speed of the compressor and the operative mode. The controller can manage three possible operative modes:

- System operating as a Ground source heat pump (GSHP). In this case, the ground is the only thermal source/sink and the refrigerant flows through valve V2 to the ground plate heat exchanger that can work as condenser or as evaporator. The conceptual model of the coupled simulation in GSHP mode is presented in Figure 3b. As the first step, the temperature of the water returning from the ground T_{BHEout} is initialized. Then, the DSHP model runs, and the heat flow rate exchanged at the ground BP-HE is calculated. The water temperature at the outlet of the ground BP-HE, $T_{DSHPout}$, is calculated with the DSHP model and used as input for the BHE model (FEFLOW® simulator). The FEFLOW® simulation runs and its output (heat flow rate exchanged with the ground and T_{BHEout}) is then used as new input data for the DSHP numerical simulation in the subsequent time step together with the updated values of the compressor speed. Since each FEFLOW® run provides many

temperature results at smaller steps, the average value in the period is taken as output for the required time. This procedure repeats for all the defined time steps and, at the end of the simulation period, the coupled simulator reports the final results in .csv format. It is worth mentioning that when the thermal load is null (compressor frequency equal to zero), the governing differential equations related to the ground and to the BHE are still solved. In this case, the boundary conditions are represented by the varying air temperature and undisturbed ground temperature.

- System operating as an Air source heat pump (ASHP). In this case, the air is the only thermal source/sink and the refrigerant absorbs/releases heat to the ambient through the finned coil heat exchanger. When operating in ASHP mode, the controller runs the DSHP model in every time step, providing as input the air temperature and compressor speed until the end of the simulation period.

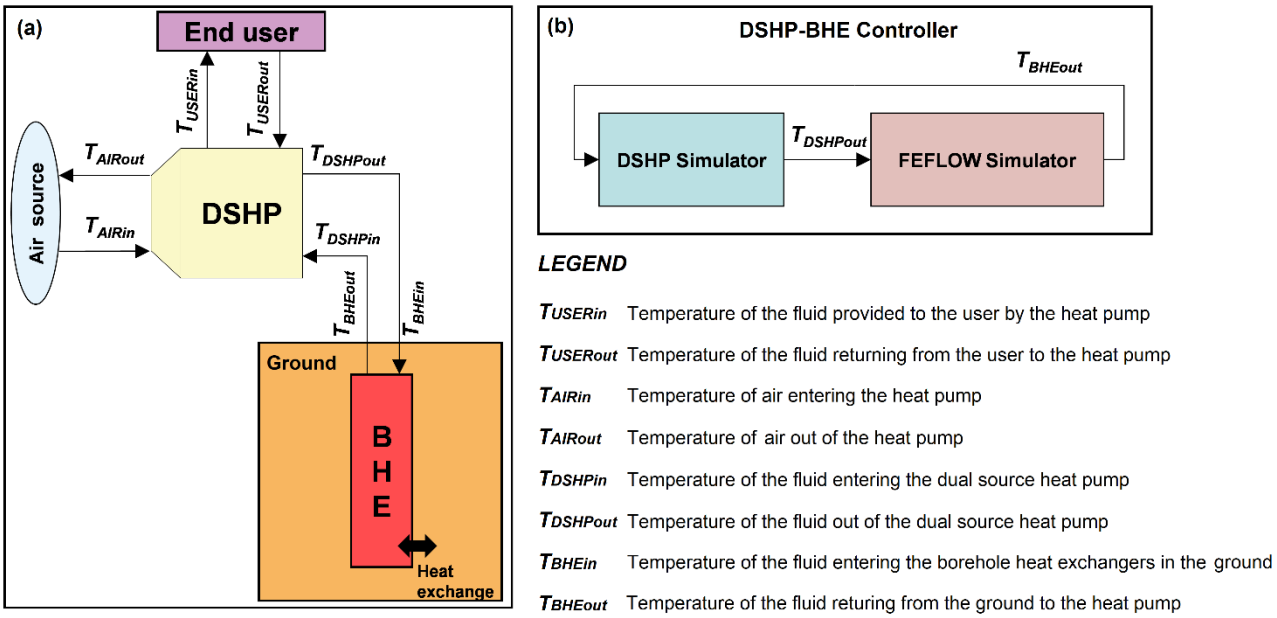

Figure 3 Conceptual model of the coupled simulation: (a) general model of the inputs and outputs of the system; (b) detail of the DSHP-BHE controller operating in GSHP mode.

- System operating as a dual source heat pump (DSHP). In this case, the workflow of the DSHP-BHE controller is presented in detail in Figure 4. The controller has to manage the switch between the ground mode and the air mode. In ground mode, the DSHP model and FEFLOW® run sequentially according to the schematic of Figure 3b. When operating in air mode, both models are run by the controller, too. The governing equations of the ground and BHE field are always solved to update the state of the ground even without working fluid circulation and if the system is operating as an ASHP. All the transient phenomena occurring in the heat pump (e.g., when the compressor is powered on or switched off) are not considered because the thermal inertia of the heat pump is negligible compared to that of the building and of the ground.

When the system operates as a DSHP, the following additional controls are also applied: the difference between the air and temperature of the fluid at the BHE outlet $T_{air} - T_{BHEout}$ is used as control parameter to decide which is the thermal source that allows to reach higher performance (more details on this are given in the Section 4.3 with a dedicated analysis); the water temperature from the BHE field (T_{BHEout}) should be higher than 4 °C otherwise the DSHP switches to air mode to avoid freezing problems (since this system should operate without glycol).

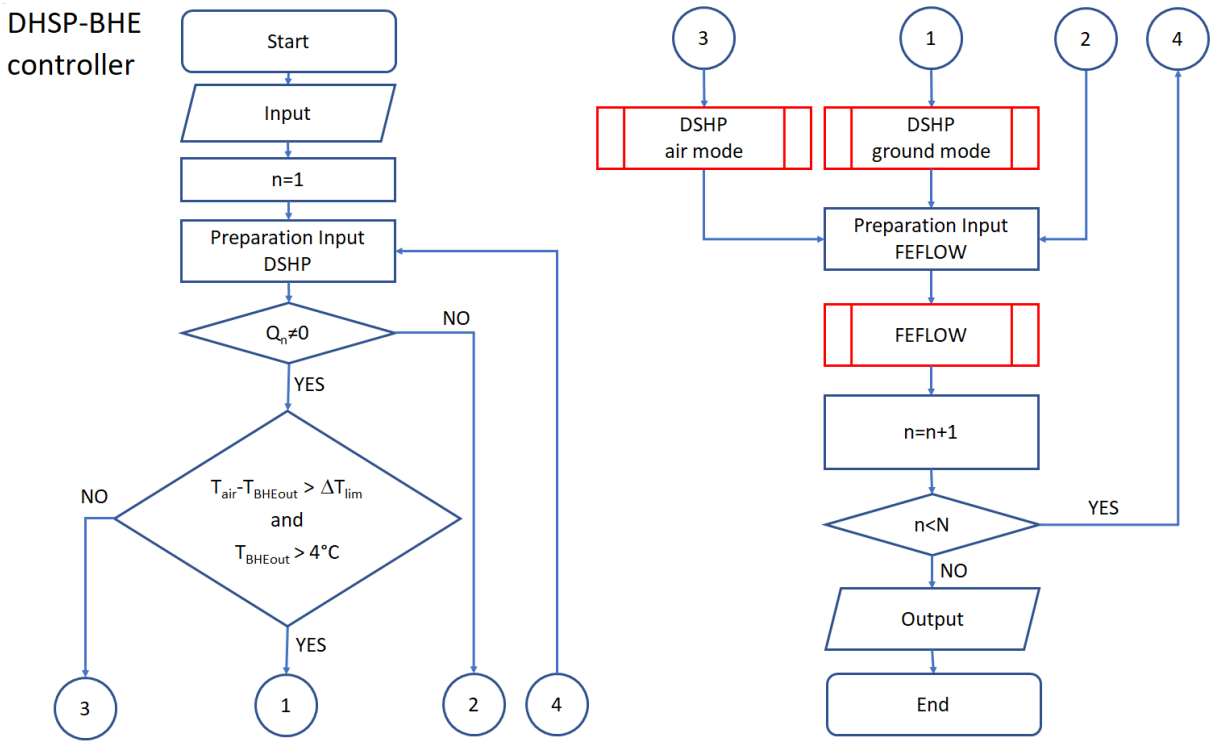

Figure 4 Workflow of the DSHP-BHE controller allowing the coupled simulation when operating in DSHP mode.

3. VALIDATION OF THE SEQUENTIAL COUPLED SIMULATOR

The model of the heat pump considering the physical equations governing the heat transfer phenomena (hereinafter "thermodynamic DSHP model") and the finite element model of the ground have been validated separately in previous works and proved to be accurate to predict the performance of the heat pump and the behaviour of the borehole heat exchanger field. The validation of the DSHP model with experimental data in several operative conditions can be found in [16]. The DSHP model was able to predict the coefficient of performance of the heat pump within ±10% both when considering heating and cooling modes. Regarding the model of the BHE implemented in FEFLOW®, multiple tests and comparisons with experimental results by many authors have shown the model to be quite robust in predicting the heat exchanged in a GSHP system (Nam et al. [35]), simulating the aquifer thermal plumes and their effect on the BHE closed-

loop applications (Rivera et al. [36]). Finally, it has been used as a benchmark for evaluating the performance of other modelling tools (Nam and Ooka [37]). Specifically to the FEFLOW® model of the CB-HE field installed in the Tribano area, the validation was performed comparing the simulated temperature changes in the ground nodes with the measured values from the monitoring points in the three observation boreholes, which can be found in [19]. The details of the model realized in FEFLOW® can be found in [34].

However, a validation of the sequential coupled model against experimental data is needed in order to calibrate the coupled model, and it is presented in this Section.

3.1 Demo site characteristics and BHE model implementation

The end-user of the dual-source heat pump system described in Section 2.1 is an office building in Tribano, located in the alluvial Po Plain (45°12′ 32′′ N 11°50′ 44′′ E). The DSHP started working in November 2017 and, after a testing period, it became fully operational in summer 2018 providing heating and cooling to the building.

The map of the system including the building, the heat pump and the CB-HE configuration is reported in Figure 5. During a preliminary monitoring activity, it has been seen that the hydraulic distribution system of the CB-HE field was not balanced since the length of the pipes between the collector and each BHE was different. Therefore, it is not possible to operate with the hypothesis of perfect distribution of the total water mass flow rate among the different probes. This specific problem has been addressed in [38] and to account for the different distributed and concentrated pressure losses, different multiplication factors are used to calculate the fraction of water mass flow rate that flows in a specific probe. The fractions of each probe are reported in Table 2.

The DSHP is instrumented and equipped with a remote controller thus all main parameters and variables of DSHP are monitored. In particular, all the temperatures and pressures at the inlet/outlet of the various components, water mass flow rates in the heat exchangers and power consumptions are acquired every 2 minutes.

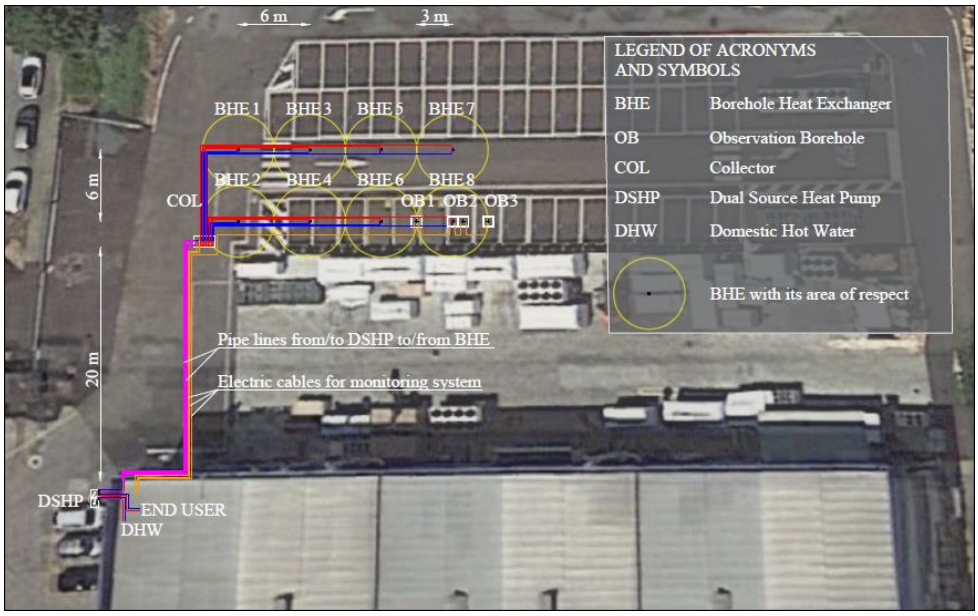

Figure 5 Map and scheme of the case study. Superimposition with Google Earth® satellite image

Borehole	CB-HE1	CB-HE2	CB-HE3	CB-HE4	CB-HE5	CB-HE6	CB-HE7	CB-HE8	TOTAL
Fraction [-]	0.142	0.193	0.116	0.142	0.101	0.116	0.09	0.101	1

Table 2 Fraction of Mass Flow Rates in the eight CB-HEs

3.2 Coupled model validation against experimental data

The validation of the coupled model has been realized considering the experimental data taken during the winter and the summer season.

As regards the winter data, five days of real system operation have been considered starting from 28th January 2019. Figure 6 reports, for the five days, the experimental heating capacity measured at the condenser (which is the thermal load required by the building) and the experimental frequency of the compressor, which is the input to the DSHP model. It can be noticed that the compressor operates mainly during the daytime, when the employees are in the office, while during the night, the compressor works mainly at the minimum frequency, equal to 30 Hz, and it turns on and off to satisfy the lower thermal demand.

The compressor frequency has been used as input to the coupled model to simulate the performance of the system during the five days with a time step equal to 30 minutes. The monitored ground temperature in the three OBs for the 28th of January has been used to reconstruct the initial state of the ground and to assign the input values to the corresponding nodes of the mesh. The temperatures in the remnant nodes have been calculated by linear interpolation. Figure 7 reports the comparison between the measured and the calculated inlet/outlet water temperature circulating

in the BP-HE condenser. The model provides accurate results and the average absolute temperature difference between the measured and simulated values is equal to 0.52 °C for the T_{BHEin} and 0.46 °C for the T_{BHEout} considering all the N time steps. The averaged absolute temperature difference has been calculated with the following equation:

$$T_d = \frac{\sum|T_{BHE-sim} - T_{BHE-meas}|}{N} \quad \text{Eq. (5)}$$

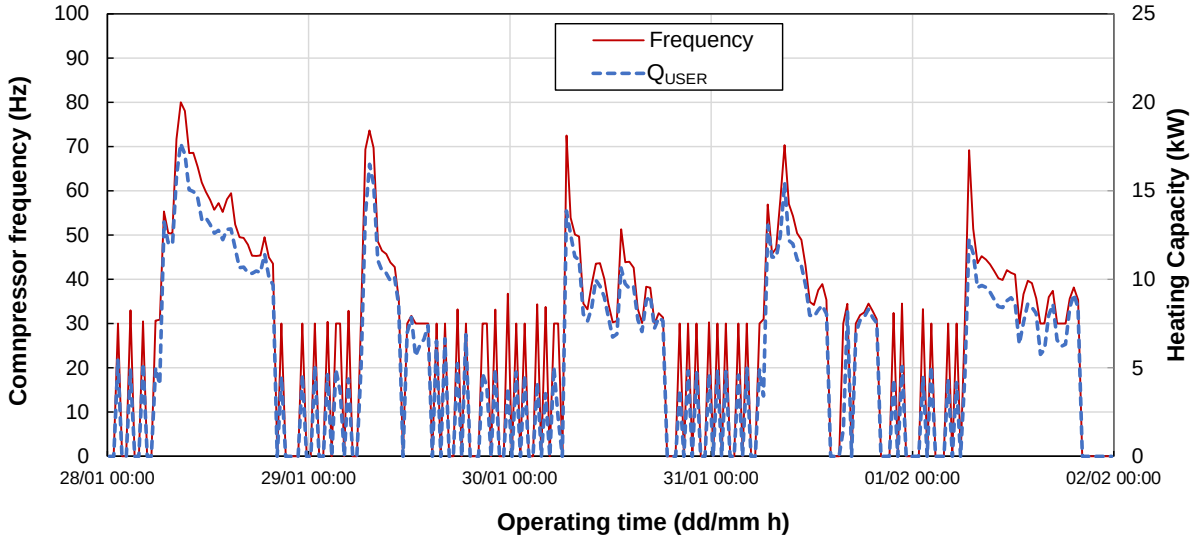

Figure 6 Frequency of the compressor and heating capacity (Q_{USER}) during the five winter days considered for the coupled simulator validation.

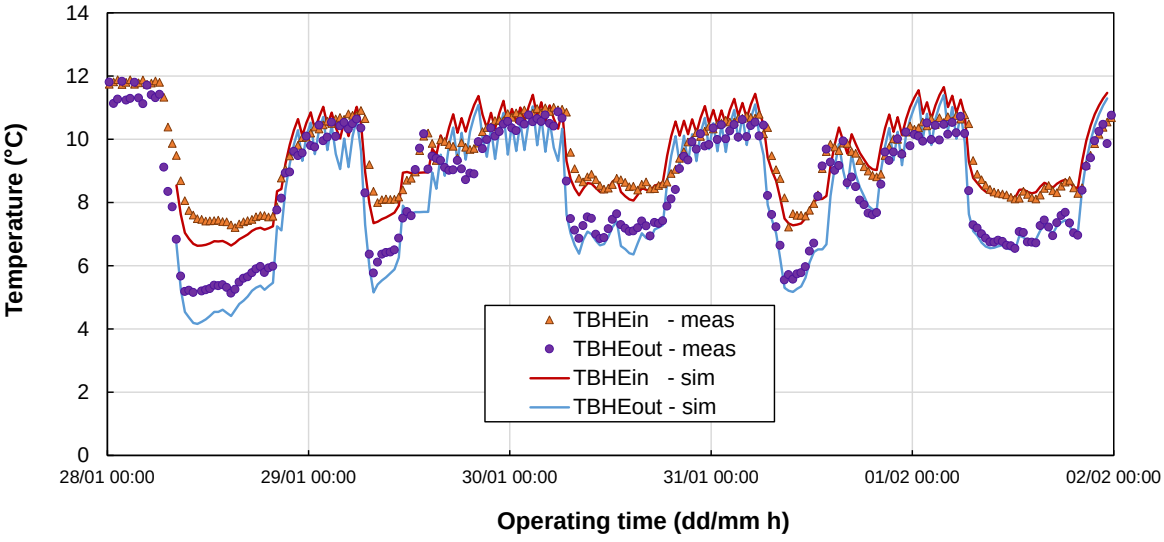

Figure 7 Comparison between experimental and numerical data of water temperature circulating in the BHE during the five winter days considered for the coupled simulator validation. Points: measured data, lines: calculated data.

The validation of the coupled DSHP-BHE model has been realized also considering the summer period (when the building requires cooling capacity for the air-conditioning system) by simulating five days of real system operation starting from the 30th of July 2019. As for the simulations in the heating period, the time step was fixed to 30 minutes and the inputs

were: the compressor frequency, the mass flow rate of water in the secondary loops, the air temperature and the temperature of the water coming from the building (considered equal to that entering the evaporator). Figure 8 displays the experimental compressor frequency and the cooling capacity at the evaporator). Similarly to the winter data, the cooling demand is higher during the daytime due to the presence of people in the office while during the night the compressor is turned off most of the time.

Figure 9 reports the comparison between the calculated and measured values of the inlet/outlet temperature of the water circulating in the BP-HE evaporator. The results were found to be in good agreement with the experimental data. In particular, the average absolute temperature difference between the measured and simulated values is equal to 0.48 °C for the T_{BHEin} and 0.99 °C for the T_{BHEout}.

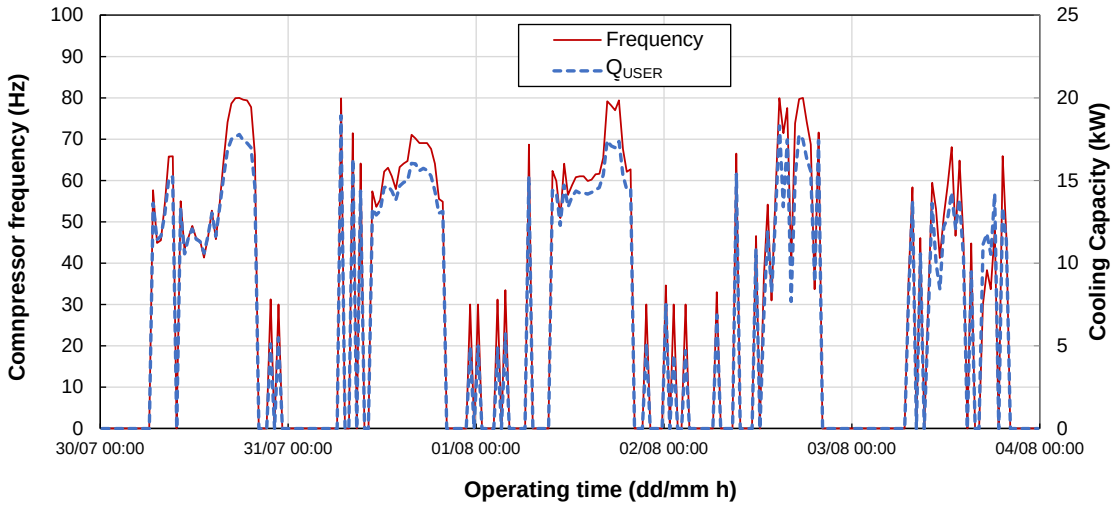

Figure 8 Frequency of the compressor and cooling capacity (Q_{USER}) during the five summer days considered for the coupled simulator validation.

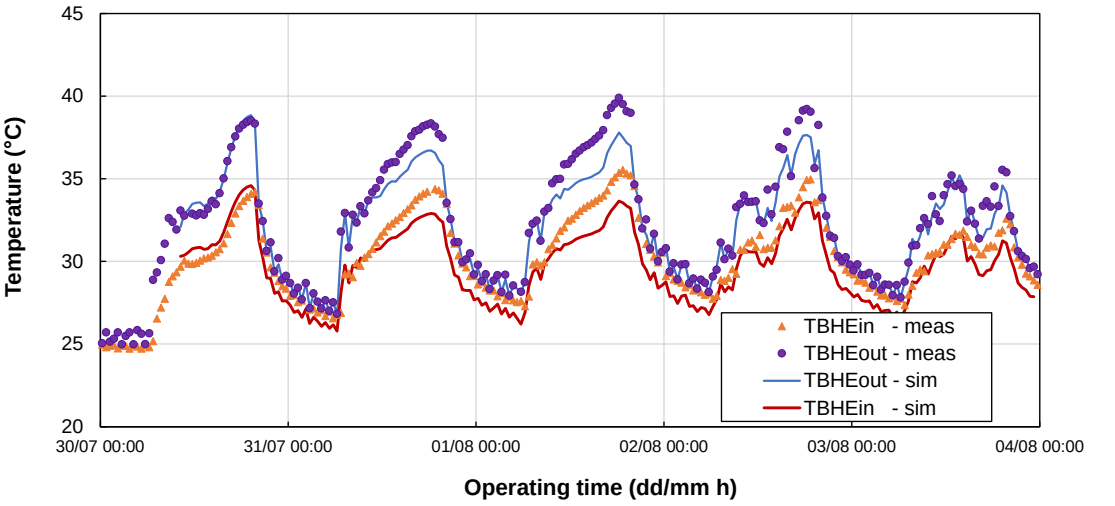

Figure 9 Comparison between experimental and numerical data of water temperature circulating in the BHE during the five summer days considered for the coupled simulator validation. Points: measured data, lines: calculated data.

3.3 Use of LUTs to reduce the simulation time

When performing yearly simulations, the coupled model is time-consuming because the DSHP model and the BHE model have to perform several iterations for each time step. In order to reduce the simulation time for the yearly calculations, the DSHP model has been used to create look-up tables (LUTs) containing the main performance indicators (i.e. heating/cooling capacity, condensation/evaporation temperatures, coefficient of performance). The LUTs have been obtained by cubic interpolation of data simulated with the DSHP model running alone. The simulations with the DSHP model have been done by varying the compressor frequency and the water temperature from the BHE. Lookup tables have been created also when the heat pump operates with the air as thermal source/sink varying the compressor frequency, the fan velocity, the air temperature and humidity. The parameters and the operational range used for the construction of the LUTs are reported in Table 3. To verify the accuracy of the LUTs, the results obtained with the DSHP model using the look-up tables have been compared with the results obtained with the DSHP model at some conditions that have not been used for LUT construction (and reported in Table 3). The results of this comparison are reported in Figure 10 in terms of cooling/heating capacity and performance coefficients (EER, COP) which are calculated as the ratio between the cooling/heating capacity Q and the heat pump power consumption P:

$$\mathrm{EER}\,,\mathrm{COP} = \frac{Q}{P} \qquad \text{Eq. (6)}$$

The data in Figure 10 refer to simulations realized at compressor speed equal to 40, 60 and 80 Hz, fan velocity equal to 60% of the maximum rate, T_{air} and $T_{DSHPout}$ equal to 30.5 °C (summer simulations) and 10.5 °C (winter simulations) respectively. It can be observed that the deviations between the results obtained with the thermodynamic DSHP model and those obtained with the LUTs are always below 1%. It can be concluded that the LUTs derived by the thermodynamic DSHP model are useful to reduce the simulation time when performing yearly simulations without sacrificing the accuracy. Thus, the results of the yearly simulations reported in Section 4 have been obtained with the LUTs.

It is important to stress that differently from the DSHP model presented in Section 2.1, the LUTs used for the yearly simulation do not take the compressor frequency as an input, but the heating or cooling power requested by the user and that has to be provided by the DSHP. All the other outputs are the same of the DSHP model, i.e. the evaporation/condensation temperature, refrigerant mass flow rate, conditions of the source fluid entering the DSHP (air or ground water), power consumptions and performance coefficients.

	Compressor frequency (Hz)	Fan velocity (%)	T_{air} Cooling (°C)	T_{air} Heating (°C)	RH_{air} (%)	$T_{BHE,out}$ Cooling (°C)	$T_{BHE,out}$ Heating (°C)
Min	30	30	25	-5	0	4	12
Max	90	90	40	25	100	20	40
Step	20	20	1	1	20	1	1

Table 3 Input range selected for the creation of the look-up tables based model of the DSHP. The table reports both the environmental conditions (air and ground water conditions) and the operative conditions of the heat pump (compressor frequency and fan speed) for the various modes (heating or cooling).

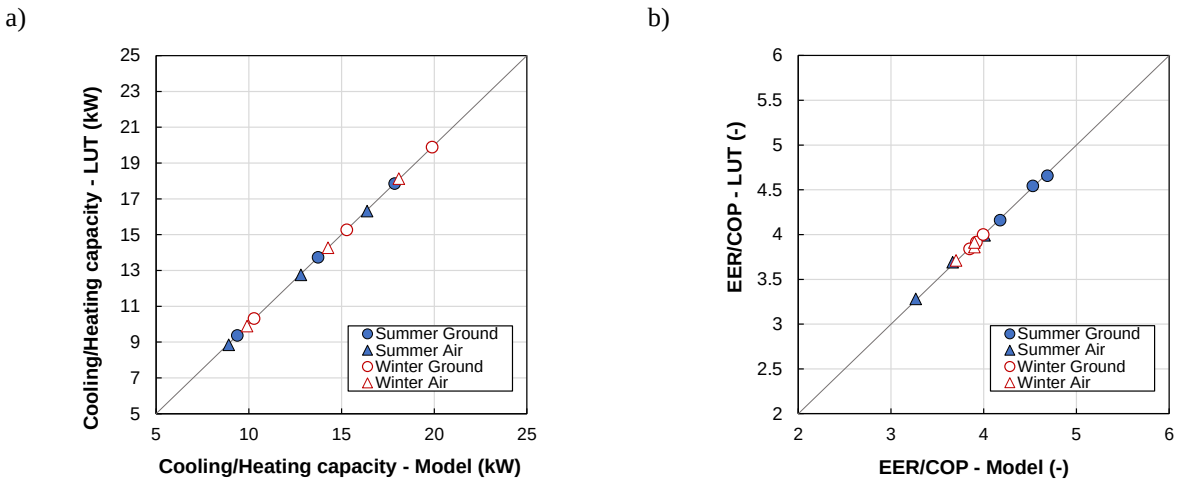

Figure 10 Comparison between the results obtained by the DSHP model and the values provided by the LUTs. Cooling/Heating capacity a) EER/COP b).

4. YEARLY SIMULATIONS

The coupled model has been used to perform yearly simulations of the functioning of the DSHP-BHE system. Since the DSHP can work both with the air or the ground as the thermal source/sink, this raises the problem of how to manage the two thermal sources to maximize the performance of the system.

4.1 Yearly simulation results: performance of the DSHP when working as an ASHP or as a GSHP

In this Section, the results of the first set of simulations are presented: these simulations have been done considering the dual-source heat pump working as an ASHP (air as the only source/sink) or as a GSHP (ground as the only source/sink) for the whole year. The simulations of the heat pump working in air mode consider the fan velocity that guarantees the maximum hourly COP of the system.

To perform the yearly simulations, the hourly weather data for the city of Tribano have been provided by the Regional Environmental Authority ARPAV [39]: the average air temperature was equal to 13.9 °C, minimum temperature equal

to -8 °C and a maximum temperature equal to 37.9 °C. The space heating of the building is supposed to work only when the external temperature is below 18 °C in the period from the beginning of November to the end of March and it is active during the daytime from 7 AM to 7 PM (12 h operation). The nominal space heating load is equal to 15 kW at the design point which is defined considering an external temperature equal to -5 °C; the thermal load decreases linearly for higher external air temperatures [40]. It is assumed that during the heating season the water enters the user heat exchanger of the heat pump at 40 °C and exits at 45 °C. The air-conditioning system of the building is supposed to work only when the external temperature is above 25 °C in the period from the beginning of May to the 15th of September during the daytime from 7 AM to 7 PM (12 h operation). The cooling load increases linearly with the external temperature from 25 °C to 38 °C, the maximum cooling load is equal to 15 kW. It is assumed that during the cooling season the water enters the user heat exchanger at 12 °C and exits at 7 °C. The minimum heating/cooling thermal load required by the building was set equal to 10 kW. The yearly simulations start from the 28th of January, when the reconstructed natural state of the ground was available and used for the model validation (see Section 3.2). When performing the ground mode simulation, the water mass flow rate on the ground loop was considered to be constant and equal to 3900 kg/h.

Figure 11 reports the air temperature T_{air} during the year and the temperature difference between the external air and the water coming from the BHE field ($T_{BHEout} - T_{air}$) calculated from the simulation with the heat pump working as GSHP. The temperature values are reported as simple moving average within 24 hours. It can be observed that during the cooling season T_{BHEout} is always lower than T_{air}, being on average 3.2 K lower. The result of this is that in the summer period the heat pump working as ASHP will be less efficient compared to the GSHP. Indeed, during the cooling season, the mean coefficient of performance obtained with the GSHP is almost twice the one obtained with the ASHP. Considering the seasonal performance factor (SPF) is defined as:

$$SPF = \frac{\sum Q_n \cdot \Delta t_n}{\sum P_n \cdot \Delta t_n} \qquad \text{Eq. (7)}$$

where $Q \cdot \Delta t$ represents the hourly cooling/heating provided by the DSHP (i.e. the thermal load Q_{USER}) and $P \cdot \Delta t$ is the corresponding energy consumption. During the cooling season, the SPF in ground mode is equal to 7.75, while in air mode is equal to 4.26.

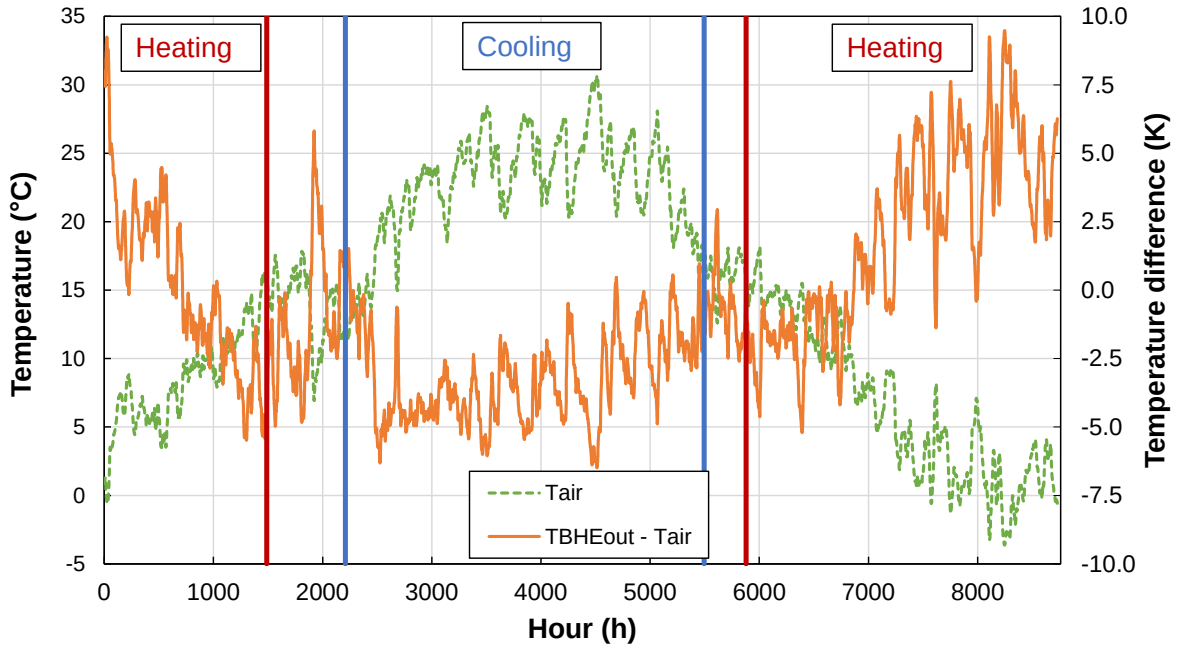

Figure 11 Air temperature during the yearly simulation (orange straight line). Difference between ground temperature (water entering the heat pump from the ground loop) and air temperature in the case of the heat pump working in GSHP mode (blue dotted line). The data reported are the simple moving average within 24 hours.

In heating mode, the mean hourly performance coefficient when the heat pump operates with the ground source is equal to 3.70 and when the air source is used, it is equal to 3.62. The seasonal performance coefficient is 9.8% higher for the GSHP compared to the ASHP (SPF=4.26 in ground mode, SPF=3.88 in air mode). However, when this system operates for the whole winter season in ground mode, T_{BHEout} tends to progressively decrease during the year reaching temperatures below the antifreeze temperature limit (less than 4 °C). This means that for the present case study of shallow borehole heat exchangers it would not be possible to work only in ground mode without using the antifreeze addition (to secure the correct and safe work of the system).

4.2 Control strategy and results of coupled simulations

As reported in the previous Section, the performance of the present heat pump prototype working in ground mode-only is higher compared to the air mode-only operation when considering the summer season (cooling period). During the winter season (heating period), the use of this undersized CB-HE field is not always convenient, leading to low water temperatures inside the BHEs. Furthermore, from Figure 11 it can be observed that in mid-season periods when heating is required, the air temperature (moving average) is higher than ground temperature by more than 2 K, meaning that the functioning in air mode can still be a valid alternative. In order to exploit both the air and the ground source, it is possible to operate in dual source mode and this will allow to achieve a double benefit:

- increase the performance of the heat pump compared to the case of working in air-only or ground-only mode.
- reduce the temperature drift of the ground and avoid low temperature of the water returning from the ground with the risk of freezing.

However, this poses the problem of how to manage the two thermal sources and to decide a control strategy to switch between them to maintain high efficiencies. The results of the simulations in air-only mode and ground-only mode have been used to develop a switching strategy for the heating season. Figure 12 reports the hourly COP difference ($COP_{air} - COP_{ground}$) as a function of the temperature difference between the two sources ($T_{air} - T_{BHEout}$) obtained from the simulations in air-only mode and ground-only mode. It can be observed that the COP difference is well correlated with the temperature difference as a linear function; on average, COP_{air} is higher than COP_{ground} when the air temperature is higher by 1.6 K than the temperature of the water returning from the BHE field. This temperature difference is an effective parameter that can be also easily implemented in the real controller of the heat pump system. Regarding the control strategy in the model, when the temperature difference reported in Eq. (8) is higher than $\Delta T_{lim} =$ 1.6 K, the heat pump operates in air mode otherwise it operates in ground mode.

$$(T_{air} - T_{BHEout}) > \Delta T_{\mathrm{lim}} \qquad \text{Eq. (8)}$$

It must be mentioned that the controller manages to switch to air mode also during the periods when the water returning from the ground reaches values less than 4 °C (T_{BHEout} < 4 °C): in this case, the objective is to avoid excessive degradation of the heat pump performance when working in ground mode and also to simulate a system where anti-freeze is not used.

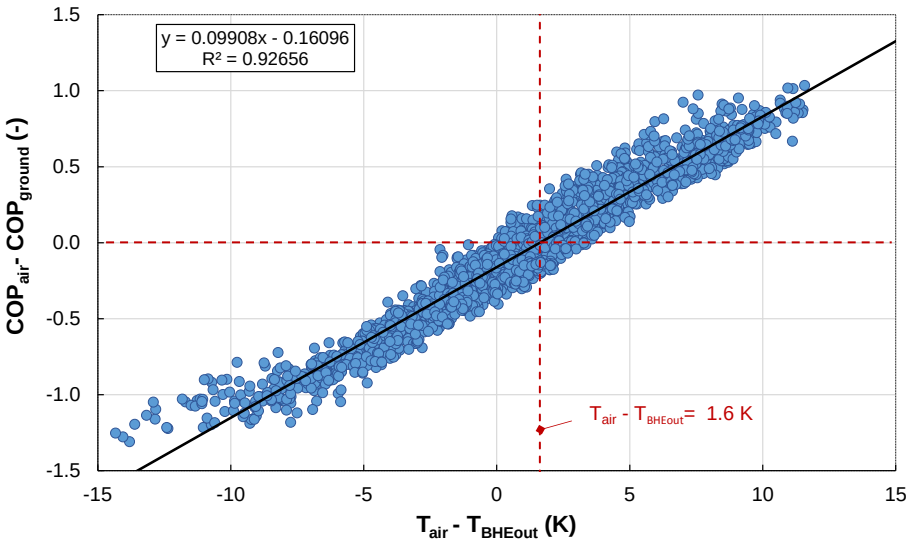

Figure 12 Difference between the hourly performance coefficients of the DSHP operating with air and ground source only against the temperature difference between the two sources ($T_{air} - T_{BHEout}$).

In the following, the results obtained with the simulation of the system working in dual-source configuration with the above-mentioned control logic (Figure 12) are reported. Figure 13 reports the evolution of the temperature of the water returning from the ground BHEs (T_{BHEout}) as simple moving average with 24 hours period during 3 years of operation. The simulation has been realized considering a time step equal to 4 h. It can be observed that after the first year, where the initial ground conditions were set starting from experimental data, the water temperature coming from the BHEs is slightly decreased but tends to follow a stable pattern without a further long-term change. The graph also reports the same result referred to the yearly simulations realized with a time step equal to 1 h for the GSHP mode only and for the DSHP operating with the same logic. It can be observed that the results obtained with the DSHP mode and different time steps (1 h for the 1-year simulation and 4 h for the three-years simulation) did not lead to remarkable variations in the temperature trends. On the contrary, if comparing the DSHP and GSHP mode, it can be observed that during the heating season the trends of the water temperature returning from the ground are substantially different. Indeed, when considering the operation of the DSHP, the variation of the ground temperature during the heating season is less sharp compared to the case of the GSHP (see Figure 13 from 5000 h to 6500 h and from 1400 h to 2500 h). In addition, Figure 14 displays the average, minimum and maximum values of $T_{DSHPout}$ obtained for the GSHP and DSHP configurations. The average water temperature obtained by the DSHP simulation results to be higher compared to the one obtained by the GSHP simulation, due to the use of the air source in the mid-season periods, reducing the use of the ground source. The operation strategy assures a temperature of the water returning from the BHEs equal to 9.9 °C during the DSHP simulation, which is more than 3 K higher than the value obtained during the GSHP simulation (equal to 6.7 °C).

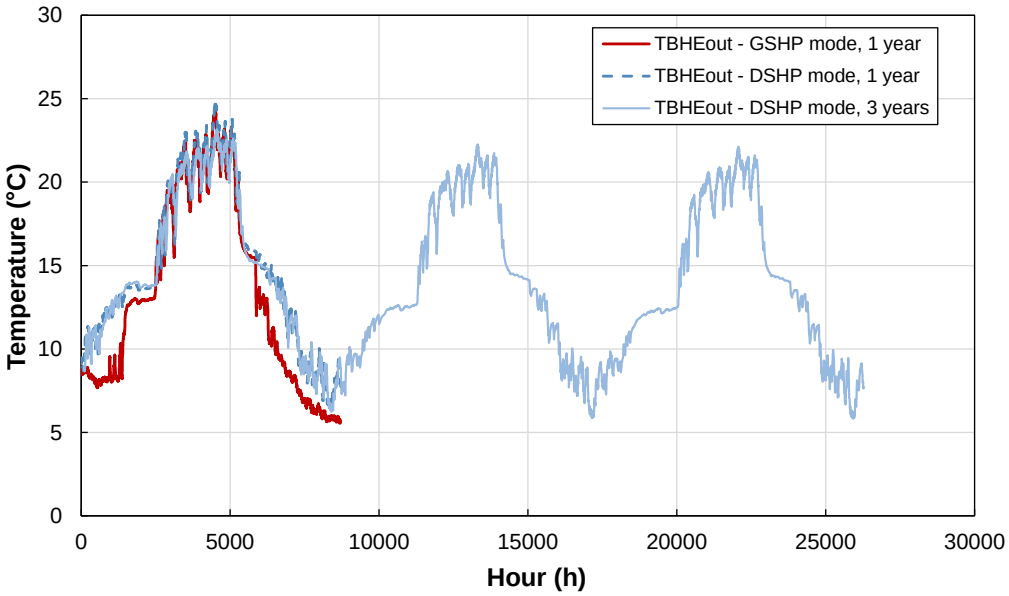

Figure 13 Temperature of the water returning from the ground (T_{BHEout}) during the three years simulation with the DSHP system (4 h time step, blue straight line), yearly simulation with the DSHP system (1 h time step, blue dotted line), yearly simulation with the GSHP system (1 h time step, red straight line). The results are reported as simple moving average with 24 hours period.

Figure 15 reports a comparison between the results of the 1-year simulations realized considering the heat pump operating with only one source/sink (as ASHP or as GSHP) and as a DSHP. Figure 15a shows the seasonal performance factor calculated according to Eq. (7) for the heating season. It has been found that the minimum SPF is obtained with the ASHP and is equal to 3.88 while the SPF is 9.8% higher in the case of GSHP operations (SPF=4.26). The SPF in the case of DSHP is equal to 4.42, thus 13.8% higher than in the case of ASHP and 3.8% higher than in the case of GSHP. This difference is due to the fact that, as suggested by Figure 13 and Figure 14, the temperature of the ground in the DSHP configuration is higher than in the ground-only operation and that the air source is used when its performance is higher. Furthermore, it was found that the ground source is used for 56% of the heating season in the DSHP configuration, whereas the air source is used for 44% of the same period (i.e. when Eq. (8) is satisfied). Two further observations can be done regarding the dual-source operation:

- During the heating period, the mean air temperature is equal to 7.6 °C, whereas the average temperature when only the air source is used (DSHP in air mode) is equal to 12 °C. This means that another advantage of this approach is the possible reduction of the defrosting cycles.
- Regarding the ground source, even if it has been mainly used during the coldest period of the heating season, the mean value of COP (equal to 3.88) was found to be 4.8% higher than in the case of the ground-only (GSHP)

operation, meaning that with the DSHP system the ground was less stressed during the coldest season and this is fundamental to preserve the ground thermal source in a long-term perspective.

In addition, the DSHP system avoids the system to reach water temperature returning from the BHE lower than 4 °C, which was not possible when working as GSHP.

Finally, Figure 15b shows the seasonal performance factor calculated according to Eq. (7) for the yearly operation: in this case, the advantage of the usage of the ground source is more prominent: compared to the ASHP (SPF=3.99), the SPF is 24.8% higher in the case of GSHP operations (SPF=4.98) and 27.9% higher in the case of DSHP operations (SPF=5.1). Therefore, the use of DSHP is even more advantageous than GSHP only, with 2.4% increase of the SPF.

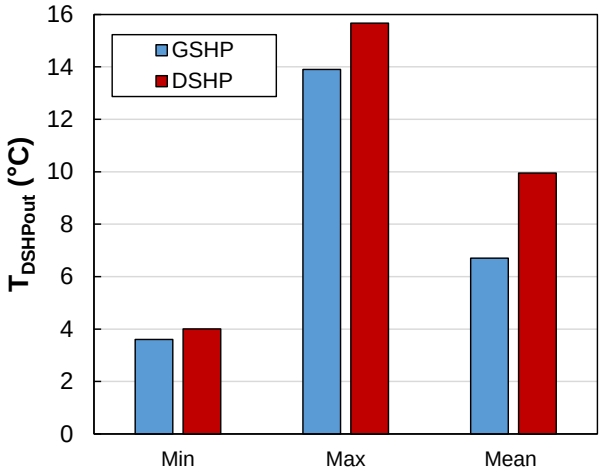

Figure 14 Calculated values of the minimum, maximum and mean water temperature at the outlet of the BHEs (T_{BHEout}) during the heating season in the case of ground-only mode (GSHP) and dual source mode (DSHP).

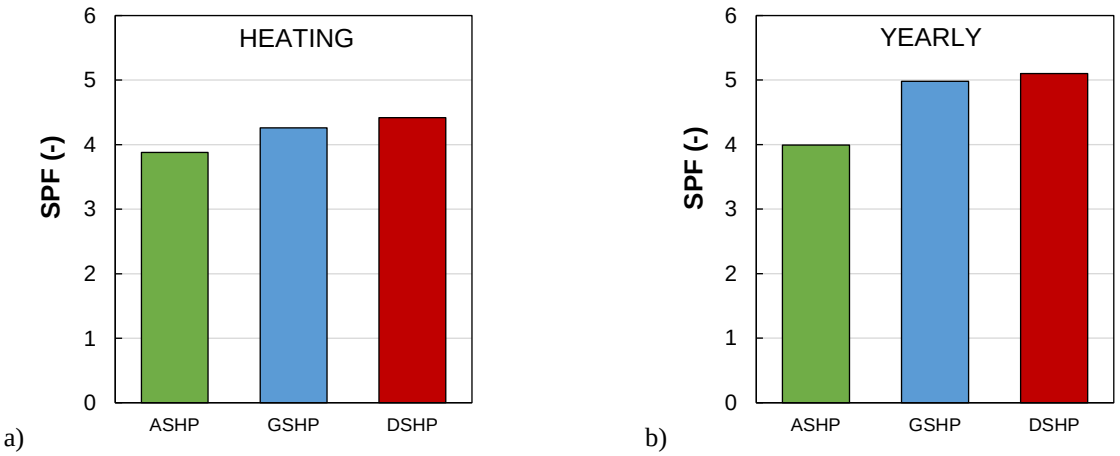

Figure 15 Seasonal performance factor obtained in the air-only mode (ASHP), ground-only mode (GSHP) and dual source mode (DSHP) during the heating season (a) and during the yearly operation (b).

5. CONCLUSIONS

In this study, a new sequential coupled model used to simulate the dynamic behaviour of a heat pump system linked to a borehole heat exchangers' field is presented. To perform the coupled simulations, an external controller has been developed in Matlab® to run consecutively two models:

- the heat pump model, which considers the physical equations that govern the heat transfer in the heat exchangers of the heat pump;
- the model of the borehole heat exchangers' field, developed using the software FEFLOW® which can operate fully transient simulations.

The coupled model can simulate several system configurations and the operations of the heat pump as an ASHP, GSHP or DSHP. The results have been compared with the experimental data obtained from the monitoring of a DSHP installed in Tribano (Italy). The analysis showed that in the winter and summer operation the average deviation between the measured and simulated water temperature entering/exiting the BHEs is below 1 K.

The validated coupled model has been used for several simulations and the main results are the followings:

- Yearly simulations of the heat pump working as an ASHP or as a GSHP have been performed. According to the simulation results: during the cooling season the GSHP can reach a SPF equal to 7.75 while the ASHP can reach a SPF equal to 4.2; during the heating season the advantage in the use of a ground source heat pump persists but reduces and the SPF is 9.8% higher compared to that of the ASHP.
- The coupled simulations highlight that when the heat pump operates entirely as a GSHP during the winter season, the heating demand is satisfied but the temperature of the water in the BHEs reaches values lower than the antifreeze limit equal to 4 °C, meaning that the borehole heat exchangers' field designed would be insufficient.
- The results of the simulations in air-only mode and ground-only mode have been used to develop a switching strategy for the heating season. In the present case, the COP operating in air mode is higher than that operating in ground mode when the temperature of the air is on average 1.6 K higher than the temperature of the water returning from the ground.
- The switching strategy between the two sources has been implemented in the controller to drive the yearly simulation of the DSHP. Considering this switching strategy, during the heating season the heat pump works with the air source for 44% of the time and the seasonal performance coefficient increases by 13.8% as compared to the air mode-only simulation and by 3.8% compared to the ground-only simulation. The

simulation proved that the addition of the air source allowed to satisfy the total energy needs, without any addition of borehole numbers or higher depth, thus with substantial investment cost savings. On the other hand, the switching strategy based on source temperature allowed to choose the best source in terms of performance, avoiding the defrost cycle in air mode and allowing a faster thermal recharge of the ground.

Finally, this paper demonstrated a new procedure to perform coupled simulations of shallow geothermal systems linked to dual-source heat pumps. Further studies will focus on the generalization of the procedure. Specifically, new simulations will be performed over different and more complex types of heat pump systems and borehole heat exchangers, with the aim to expand the number of potential applicants and end-users.

ACKNOWLEDGEMENTS

The research was supported also by the research project GEOTeCH [17], co-funded by the European Community Horizon 2020 Program for European Research and Technological Development (2014–2020) – Grant Agreement 656889. The support of Hiref S.p.A. is also acknowledged.

NOMENCLATURE

A	Area	[m^2]
ASHP	Air-source heat pump	
BP-HE	Brazed plate heat exchanger	
CB-HE, BHE	Coaxial borehole/borehole heat exchanger	
COP	Coefficient of performance	[-]
DSHP	Dual-source heat pump	
EER	Energy efficiency ratio	[-]
FC-HE	Finned coil heat exchanger	
GSHP	Ground-source heat pump	
$GWP_{100years}$	Global Warming Potential over 100 years	
HTC	Heat transfer coefficient	[W m^{-2} K^{-1}]
$\dot{m}$	Mass flow rate	[kg s^{-1}]
N	Total number of time steps	[-]
NTU	Number of Transfer Units	[-]
OB	Observation Borehole	
P	Heat pump consumption	[W]
Q	Heat flow rate, heating/cooling capacity	[W]
R	Thermal resistance	[m^2 K W^{-1}]
SC	Subcooling	[K]
SH	Superheating	[K]
SPF	Seasonal performance factor	[-]
T	Temperature	[°C]
Tol	Tolerance value for convergence	[K]
U	Global heat transfer coefficient	[W m^{-2} K^{-1}]
Δt	Time step	[s]

ΔT_{lim}	Limit temperature difference	[K]
ΔT_{ml}	Logarithmic mean temperature difference	[K]

Subscripts

air, AIR	Air
BHE	Borehole heat exchanger side
BP	Brazed plate
C	Condenser, water side
Cd	Conduction
Cond	Condenser
D	Difference
E	Evaporator, water side
Evap	Evaporator
GUESS	Guess/initial value
I	Heat exchanger discretization
In	Inlet
J	BP-HE discretization
Lim	Limit
Max	Maximum
Meas	Measured
n	Time step
N	Total number of time steps
NEW	New/updated value
Out	Outlet
R	Refrigerant
Re	BP-HE region
Sim	Simulated
USER	User side

Greek symbols

E	FC-HE effectiveness	[-]
η_{comp}	Compressor efficiency	[-]

REFERENCES

1. Kavanaugh, S.P.; Rafferty, K. Design of geothermal systems for commercial and institutional buildings. *ASHRAE Trans.* **1997**.
2. Focaccia, S.; Tinti, F.; Monti, F.; Amidei, S.; Bruno, R. Shallow geothermal energy for industrial applications: A case study. *Sustain. Energy Technol. Assessments* **2016**.
3. Cui, Y.; Zhu, J.; Twaha, S.; Riffat, S. A comprehensive review on 2D and 3D models of vertical ground heat exchangers. *Renew. Sustain. Energy Rev.* 2018.
4. Al-Khoury, R.; Kölbel, T.; Schramedei, R. Efficient numerical modeling of borehole heat exchangers. *Comput. Geosci.* **2010**.
5. Javed, S.; Claesson, J. New analytical and numerical solutions for the short-term analysis of vertical ground heat exchangers. In Proceedings of the ASHRAE Transactions; 2011.
6. Pasquier, P.; Marcotte, D. Short-term simulation of ground heat exchanger with an improved TRCM. *Renew. Energy* **2012**.
7. Ruiz-Calvo, F.; De Rosa, M.; Acuña, J.; Corberán, J.M.; Montagud, C. Experimental validation of a short-term Borehole-to-Ground (B2G) dynamic model. *Appl. Energy* **2015**.
8. Li, X.; Lyu, W.; Ran, S.; Wang, B.; Wu, W.; Yang, Z.; Jiang, S.; Cui, M.; Song, P.; You, T.; et al. Combination principle of hybrid sources and three typical types of hybrid source heat pumps for year-round efficient operation. *Energy*

2020, *193*.
9. Grossi, I.; Dongellini, M.; Piazzi, A.; Morini, G.L. Dynamic modelling and energy performance analysis of an innovative dual-source heat pump system. *Appl. Therm. Eng.* **2018**, *142*, 745–759.
10. Lazzarin, R.; Noro, M. Photovoltaic/Thermal (PV/T)/ground dual source heat pump: Optimum energy and economic sizing based on performance analysis. *Energy Build.* **2020**.
11. De Rosa, M.; Ruiz-Calvo, F.; Corberán, J.M.; Montagud, C.; Tagliafico, L.A. A novel TRNSYS type for short-term borehole heat exchanger simulation: B2G model. *Energy Convers. Manag.* **2015**.
12. Hein, P.; Kolditz, O.; Görke, U.J.; Bucher, A.; Shao, H. A numerical study on the sustainability and efficiency of borehole heat exchanger coupled ground source heat pump systems. *Appl. Therm. Eng.* **2016**.
13. Li, C.; Mao, J.; Zhang, H.; Xing, Z.; Li, Y.; Zhou, J. Numerical simulation of horizontal spiral-coil ground source heat pump system: Sensitivity analysis and operation characteristics. *Appl. Therm. Eng.* **2017**.
14. Corberán, J.M.; Cazorla-Marín, A.; Marchante-Avellaneda, J.; Montagud, C. Dual source heat pump, a high efficiency and cost-effective alternative for heating, cooling and DHW production. *Int. J. Low-Carbon Technol.* **2018**, *13*, 161–176.
15. Diersch, H.J.G.; Bauer, D.; Heidemann, W.; Rühaak, W.; Schätzl, P. Finite element modeling of borehole heat exchanger systems. Part 2. Numerical simulation. *Comput. Geosci.* **2011**.
16. Zanetti, E.; Azzolin, M.; Bortolin, S.; Busato, G.; Del Col, D. Experimental data and modelling of a dual source reversible heat pump equipped with a minichannels evaporator. *Therm. Sci. Eng. Prog.* **2022**.
17. GEOTECH - Geothermal Technology for €conomic Cooling and Heating. Available online: https://cordis.europa.eu/project/id/656889.
18. IPCC *Climate Change 2014: Synthesis Report. Contribution of Working Groups I, II and III to the Fifth Assessment Report of the Intergovernmental Panel on Climate Change*; 2014; ISBN 9789291691432.
19. Tinti, F.; Carri, A.; Kasmaee, S.; Valletta, A.; Segalini, A.; Bonduà, S.; Bortolotti, V. Ground temperature monitoring for a coaxial geothermal heat exchangers field: Practical aspects and main issues from the first year of measurements. *Rud. Geol. Naft. Zb.* **2018**.
20. Rich, D.G. Effect of Fin Spacing on the Heat Transfer and Friction Performance of Multi-Row, Smooth Plate Fin-and-Tube Heat Exchangers. *ASHRAE Trans.* **1973**, *79*, 137–145.
21. Pichtel, J. *Handbook of Chemical and Environmental Engineering Calculations*; 2003; Vol. 32; ISBN 0071433260.
22. Cavallini, A.; Del Col, D.; Doretti, L.; Matkovic, M.; Rossetto, L.; Zilio, C.; Censi, G. Condensation in horizontal smooth tubes: A new heat transfer model for heat exchanger design. In Proceedings of the Heat Transfer Engineering; 2006; Vol. 27, pp. 31–38.
23. Azzolin, M.; Berto, A.; Bortolin, S.; Del Col, D. Condensation heat transfer of R1234ze(E) and its A1 mixtures in small diameter channels | Transfert de chaleur par condensation du R1234ze(E) et de ses mélanges A1 dans des canaux de faible diamètre. *Int. J. Refrig.* **2022**, *137*, 153–165.
24. Azzolin, M.; Bortolin, S. Condensation and flow boiling heat transfer of a HFO/HFC binary mixture inside a minichannel. *Int. J. Therm. Sci.* **2021**.
25. Matkovic, M.; Cavallini, A.; Del Col, D.; Rossetto, L. Experimental study on condensation heat transfer inside a single circular minichannel. *Int. J. Heat Mass Transf.* **2009**, *52*, 2311–2323.
26. Liu, Z.; Winterton, R.H.S. A general correlation for saturated and subcooled flow boiling in tubes and annuli, based on a nucleate pool boiling equation. *Int. J. Heat Mass Transf.* **1991**, *34*, 2759–2766.
27. Webb, R.L. Convective condensation of superheated vapor. *J. Heat Transfer* **1998**, *120*, 418–421.
28. Martin, H. A theoretical approach to predict the performance of chevron-type plate heat exchangers. *Chem. Eng. Process. Process Intensif.* **1996**, *35*, 301–310.
29. Longo, G.A.; Righetti, G.; Zilio, C. A new computational procedure for refrigerant condensation inside herringbone-type Brazed Plate Heat Exchangers. *Int. J. Heat Mass Transf.* **2015**, *82*, 530–536.
30. Amalfi, R.L.; Vakili-Farahani, F.; Thome, J.R. Flow boiling and frictional pressure gradients in plate heat exchangers. Part 2: Comparison of literature methods to database and new prediction methods. *Int. J. Refrig.* **2016**, *61*, 185–203.
31. EN-12900:2013. Refrigerant compressors. Rating conditions, tolerances and presentation of manufacturer's performance data. **2013**.
32. Al-Khoury, R.; Bonnier, P.G.; Brinkgreve, R.B.J. Efficient finite element formulation for geothermal heating systems. Part I: Steady state. *Int. J. Numer. Methods Eng.* **2005**.
33. Al-Khoury, R.; Bonnier, P.G. Efficient finite element formulation for geothermal heating systems. Part II: Transient. *Int. J. Numer. Methods Eng.* **2006**.
34. Tinti, F.; Azzolin, M.; Bonduà, S.; Zanetti, E.; Bortolin, S.; Busato, G.; Focaccia, S.; Marín, A.C.; Bortolotti, V. Sequential coupled simulation of a dual source heat pump and shallow geothermal reservoir. In Proceedings of the European Geothermal Congress; 2019; pp. 11–14.
35. Nam, Y.; Ooka, R.; Hwang, S. Development of a numerical model to predict heat exchange rates for a ground-

source heat pump system. *Energy Build.* **2008**.
36. Rivera, J.A.; Blum, P.; Bayer, P. Analytical simulation of groundwater flow and land surface effects on thermal plumes of borehole heat exchangers. *Appl. Energy* **2015**.
37. Nam, Y.; Ooka, R. Numerical simulation of ground heat and water transfer for groundwater heat pump system based on real-scale experiment. *Energy Build.* **2010**.
38. Cazorla-Marín, A.; Montagud-Montalvá, C.; Tinti, F.; Corberán, J.M. A novel TRNSYS type of a coaxial borehole heat exchanger for both short and mid term simulations: B2G model. *Appl. Therm. Eng.* **2020**.
39. ARPAV Agenzia Regionale per la Prevenzione e Protezione Ambientale del Veneto. Available online: https://www.arpa.veneto.it/.
40. Azzolin, M.; Cattelan, G.; Dugaria, S.; Minetto, S.; Calabrese, L.; Del Col, D. Integrated CO2 systems for supermarkets: Field measurements and assessment for alternative solutions in hot climate. *Appl. Therm. Eng.* **2021**.